

# Plastic hinge modeling of reinforced concrete Beam-Column joints using artificial neural networks

Nirmala Suwal, Serhan Guner\*

Department of Civil and Environmental Engineering, University of Toledo, Toledo, OH, 43607, USA

## ARTICLE INFO

### Keywords:

Artificial neural networks  
Beam-column joints  
Bond slip  
Global frame analysis  
Joint spring  
Lumped plasticity  
Moment-rotation  
Plastic hinge  
Shear strength  
Shear stress-strain

## ABSTRACT

Beam-column joints play a critical role in transferring forces between beam and column elements and maintaining structural integrity during severe loading. While the nonlinear behaviors of beams and columns are commonly modeled in global frame analyses through the use of plastic hinges, the behavior of joints is often omitted through the use of rigid end offsets. The objective of this study is to develop an artificial neural network and derive the plastic hinge curves required for modeling reinforced concrete beam-column joints in global frame analyses. In pursuit of this objective, a feed-forward artificial neural network (FFNN) is developed to predict the shear strengths of beam-column joints. A comprehensive dataset of 598 experimental joint specimens is compiled from 153 previously published research studies. The 555 data points, which passed the exploratory data analysis, are used to train, test, and validate the proposed network for applicability to a wide range of input variables and joint configurations. The accuracy and reliability of the proposed FFNN are evaluated using a comprehensive set of evaluation metrics in comparison with three existing networks from the literature. The proposed FFNN is used to derive the shear stress-strain and moment-rotation curves required for defining joint hinges in global frame analyses. In addition, a spreadsheet tool is developed to execute the network formulations, calculate the joint shear strength, and derive the joint hinge curves for the use of engineers and researchers.

## 1. Introduction

Reinforced concrete beam-column joints may undergo severe deformations leading to local damage, or, in extreme cases, failures affecting the integrity of an entire frame structure [1]. The main phenomena affecting the behavior of joints are the shear and bond slip deformations in the joint core. In addition, joint deformations are a major contributor to lateral story drifts [2] which places another demand on the frame. While the nonlinear behaviors associated with beams and columns are commonly accounted for in global frame analyses, the behavior of joints is often neglected through the use of rigid end offsets or other techniques that suppress joint deformations.

The primary failure modes associated with joints include the joint shear and bond slip failures [3,4]. The joint shear failure occurs when the shear stress in the joint core exceeds its shear capacity, leading to diagonal cracking of the joint core as shown in Fig. 1a [5]. The bond slip failure occurs when a set of reinforcing bars embedded in or passing through a joint core cannot develop the required bond strength with the surrounding concrete, leading to bar slippage and separation of the

beam from the joint core as shown in Fig. 1b [6]. Joint failures may also take place in combination with the beam and column failure modes that may include flexural and shear failure modes as shown in Fig. 1c [7].

Reinforced concrete frames are commonly modeled using one-dimensional frame elements based on the plastic hinge approach. This approach requires defining a plastic hinge in the form of a spring with a pre-defined force-deformation behavior. This behavior is typically idealized with multi-linear curves having pre-defined points such as cracking, yielding, maximum, and failure. There are well-defined procedures for deriving the beam and column hinge curves to model the nonlinear behavior and failure modes of beams and columns [8]. Many commonly used frame analysis tools employ these procedures to automatically derive the beam and column hinge curves [9]. Modeling the behavior of beam-column joints, however, is more complex and there is no well-defined process or an automated joint hinge calculation in most common frame analysis tools.

Modeling techniques for beam-column joints range from simple link elements [10] or rotational spring models [11–16] to more elaborate component models [17–20] and finite element models [21,22].

\* Corresponding author.

E-mail addresses: [nirmala.suwal@rockets.utoledo.edu](mailto:nirmala.suwal@rockets.utoledo.edu) (N. Suwal), [serhan.guner@utoledo.edu](mailto:serhan.guner@utoledo.edu) (S. Guner).

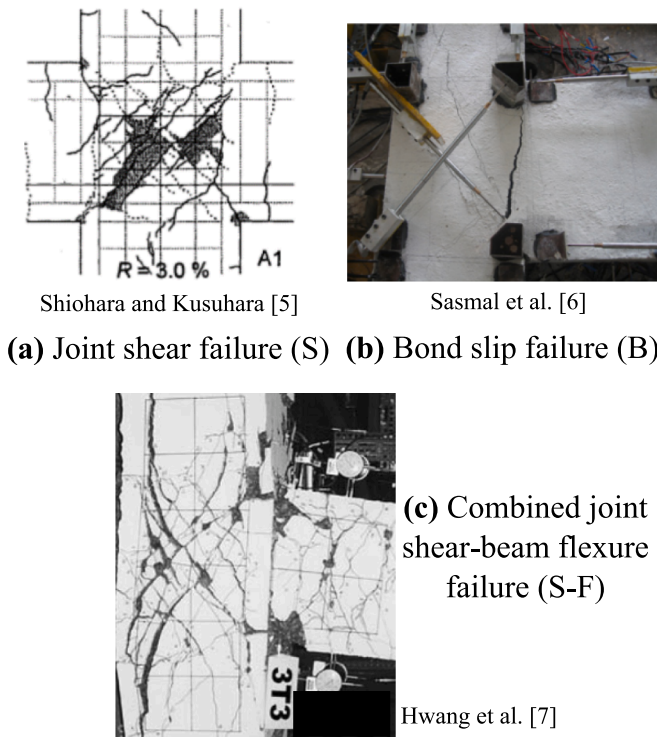


Fig. 1. Potential failure modes in beam-column joints.

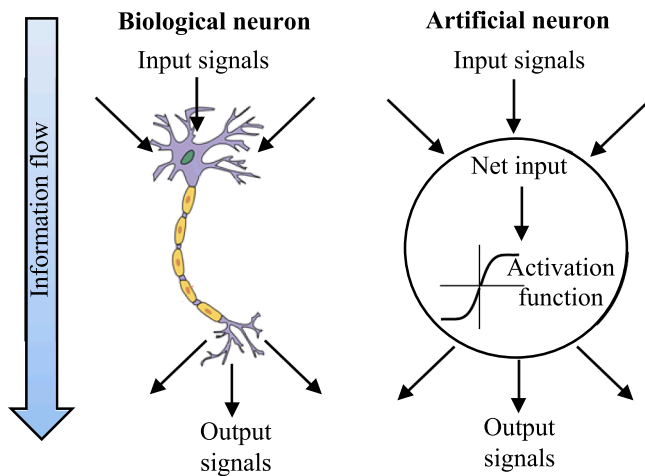


Fig. 2. Biological and artificial neurons [23].

Implementation of rotational springs in the joints of a global frame model is simple; however, the derivation of spring curves, in the form of stress-strain or moment-rotation relations, are challenging. There are many studies and formulations that can be used to derive the spring properties, but each set of formulations is empirically derived based on the experimental testing of a handful of beam-column specimens. Consequently, each set of formulations is valid for the joint configurations included in the experimental tests used to derive the formulations. There are many different joint configurations due to the large number of parameters required for defining a joint – as an example, this study uses 13 parameters to define a beam-column joint. This creates a major challenge for finding formulations that are valid for the joint configurations being modeled, and, in many cases, valid joint formulations may not be found.

This study aims to develop an artificial neural network (ANN) to

predict the joint shear strength with high accuracy and for a wide range of joint configurations. The network is trained, tested, and validated with more than 500 experimental beam-column joint specimens representing a large range of parameters. The developed formulations are implemented into a spreadsheet tool to enable practicing engineers to easily derive the shear stress-strain and moment-rotation curves for inputting into a global frame analysis model.

## 2. Review of existing literature

An ANN consists of interconnected cells called neurons. Neurons modify themselves based on the information flowing through them, mimicking the learning process of biological neurons in the human brain (Fig. 2). Each neuron receives an input signal and plugs it into a mathematical function. This function is called an activation function. The role of this function is to convert the net input into the output of the neuron, also called ‘output signal’. The output signals are modified by scalar values called ‘weights’ and ‘biases’ and then forwarded to the neurons in the subsequent layer. The neurons at the final layer output the ANN predictions.

A typical ANN will initially have random weights and biases with small values (e.g., between 0 and 1), which will lead to inaccurate results. To increase its accuracy, the ANN needs to be trained so that the weights and biases are adjusted to give more accurate results. Training of the ANN allows it to find approximate solutions to complex problems that would be challenging to solve with conventional techniques. The main types of ANNs are feed-forward, radial basis, Kohonen self-organizing, recurrent, convolutional, and modular. The feed-forward neural networks (FFNNs), which are used in this study, are one of the simplest types of ANNs. Conventional FFNNs consist of an input layer, one (and only one) hidden layer, and one output layer while deep FFNNs have multiple hidden layers. Their name comes from the information flow which always goes in one direction, from inputs to outputs (i.e., forward). More information on the types and formulations of ANNs can be found in Almeida and Guner [23].

A number of studies explored the use of ANNs for the prediction of beam-column joint shear strengths and failure modes. Kotsovu et al. [24] used an ANN to evaluate the shear capacity of exterior beam-column joints based on a database of 153 specimens. This ANN achieved a mean of 0.99 and standard deviation of 6.4 % for the predicted-to-experimental shear strengths which were shown to be significantly better than the values obtained from the design codes such as ACI 318 [8], EC2 [25], and EC8 [26]. Gao and Lin [27] explored various machine learning methods, including an ANN, to predict the failure modes of interior beam-column joints based on a database of 580 experimental specimens. They found that the ANN predicted the correct failure mode for 77 % of the specimens. Alagundi and Palanisamy [28] proposed an ANN to predict the shear strength of exterior beam-column joints and compared its performance to the empirical equations from various design codes. This ANN was developed based on a limited experimental database of 75 specimens and provided a mean of 1.05 for the predicted-to-experimental shear strength ratios; the standard deviation was not reported. To remedy the limitations of the aforementioned models, Haido [29] proposed an ANN to predict the shear strengths of both exterior and interior joints and compared its performance with empirical formulations and the values obtained from various design codes. This ANN was developed based on a database of 200 experimental specimens. Compared to the design code equations, this model demonstrated better accuracy with a mean of 0.97 and a standard deviation of 24.1 % for the predicted-to-experimental shear strength ratios. Marie et al. [30] compared six machine learning methods, including ordinary least squares (OLS), support vector machine (SVM), k-nearest neighbor (KNN), multivariate adaptive regression splines (MARS), ANN, and kernel regression, to predict the shear strengths of both interior and exterior beam-column joints. The experimental database included 98 specimens with and without transverse reinforcement. This ANN

predicted the joint shear strengths with a mean ratio of 0.96 for the predicted-to-experimental shear strength ratios; the standard deviation was not reported.

These studies demonstrate the successful applications of ANNs for predicting the beam-column joint shear strengths. This current study aims to develop an ANN with higher accuracy and more general applicability, including exterior and interior joints with or without transverse reinforcement. The end goal is to use this network to derive the joint spring curves that can be readily used in a global frame analysis model for capturing the behavior of the joint.

### 3. Proposed feed-forward neural network (FFNN)

A feed-forward neural network is developed to predict the shear stress that would cause the failure of the joint, termed as the shear strength. The main components of this network include the training algorithm, activation functions, prediction error, optimization function, learning rate, network configuration, and number of iterations. A feed-forward algorithm, with the supervised back-propagation technique, is used for the training.

The input values ( $x$ ) in the input layer are modified by weights ( $w$ ) and biases ( $b$ ) associated with each neuron using Eq. (1). The resulting net input ( $u$ ) is modified by the activation function, in Eq. (2), to produce the output ( $y$ ). A sigmoid function is chosen as the activation function because it is smooth and differentiable over its entire length and has been used successfully in previous applications [23,31–33]. Once the output is predicted by the network, the mean squared error (MSE) is calculated for  $n$  data points, as defined in Eq. (3), between the predicted ( $\tau_{pred}$ ) and experimental ( $\tau_{exp}$ ) shear strengths. The back propagation is performed to minimize the MSE by propagating it from the output layer back through the network to the input layer.

$$u = \sum (wx + b) \quad (1)$$

$$y = \frac{1}{1 + e^{-u}} \quad (2)$$

$$MSE = \frac{1}{n} \sum (\tau_{pred} - \tau_{exp})^2 \quad (3)$$

Adaptive moment estimation (Adam) [34] is used as an optimization function to update the weights and biases according to Eqs. (4) and (5), respectively, with a learning rate ( $k$ ) of 0.01. This allows the weights and biases to converge to optimum values with less iterations (i.e., faster) while providing more accurate shear strength predictions. Adam uses the stochastic momentum for gradient descent [35] ( $V_d$ ) along with the root mean square propagation ( $\sqrt{S_d + \epsilon}$ ) [36].

$$w = w - k \frac{V_{dw}}{\sqrt{S_{dw} + \epsilon}} \quad (4)$$

$$b = b - k \frac{V_{db}}{\sqrt{S_{db} + \epsilon}} \quad (5)$$

where  $V_{dw}$  and  $V_{db}$  represent the  $V_d$  terms related to the weights and biases, respectively. Similarly,  $\sqrt{S_{dw} + \epsilon}$  and  $\sqrt{S_{db} + \epsilon}$  represent the  $\sqrt{S_d + \epsilon}$  terms related to the weights and biases, respectively.

The stochastic momentum gradient descent ( $V_d$ ) accelerates the convergence speed of a stable FFNN by building up velocity in consistent gradient directions over time. This gradient is determined by the derivative of the MSE with respect to the weights or biases. For  $t$  number of iterations,  $V_d$  is expressed in Eq. (6) for weights and Eq. (7) for biases, where  $\beta$  is a constant taken as 0.9.

$$V_{dwt} = \beta V_{dwt(t-1)} + (1 - \beta) \frac{dMSE}{dw} \quad (6)$$

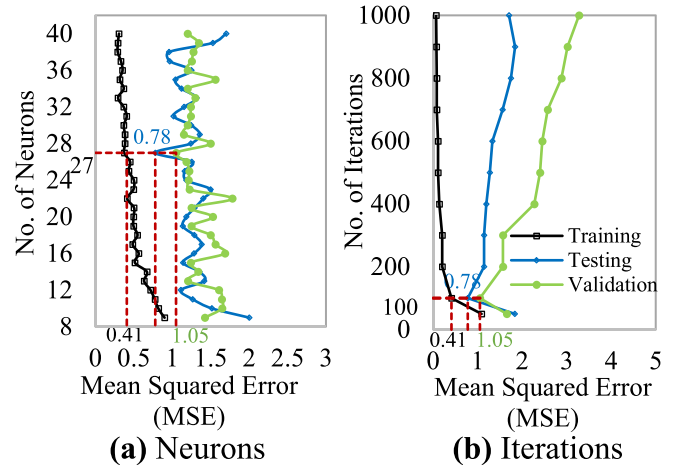


Fig. 3. MSEs computed for various network configurations and number of iterations.

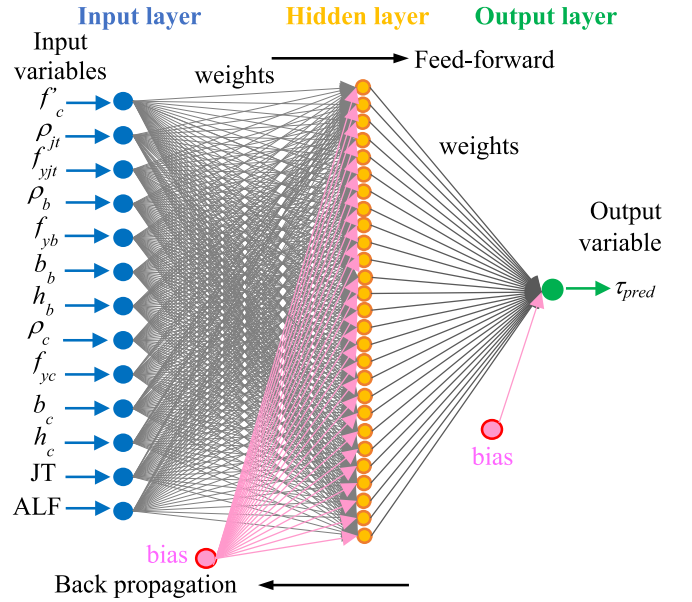


Fig. 4. Proposed network configuration.

$$V_{dbt} = \beta V_{dbt(t-1)} + (1 - \beta) \frac{dMSE}{db} \quad (7)$$

where  $V_{dwt}$  and  $V_{dbt}$  represent the  $V_d$  terms related to the weights and biases for the  $t^{\text{th}}$  iteration, and  $V_{dwt(t-1)}$  and  $V_{dbt(t-1)}$  represent the  $V_d$  terms related to the weights and biases for  $(t-1)^{\text{th}}$  iterations.

The root-mean-square propagation ( $\sqrt{S_d + \epsilon}$ ) has the ability to adjust the learning rate based on the historical gradients and improve the convergence speed. For  $t$  number of iterations, the term ( $S_d$ ) is expressed in Eq. (8) for weights and Eq. (9) for biases. The term  $\epsilon$  is introduced to avoid the division-by-zero error. A small value in the range of  $10^{-8}$  to  $10^{-10}$  may be used for  $\epsilon$ . In this study, the value of  $10^{-8}$  is used.

$$S_{dwt} = \beta S_{dwt(t-1)} + (1 - \beta) \left( \frac{dMSE}{dw} \right)^2 \quad (8)$$

$$S_{dbt} = \beta S_{dbt(t-1)} + (1 - \beta) \left( \frac{dMSE}{db} \right)^2 \quad (9)$$

where  $S_{dwt}$  and  $S_{dbt}$  represent the  $S_d$  terms related to the weights and

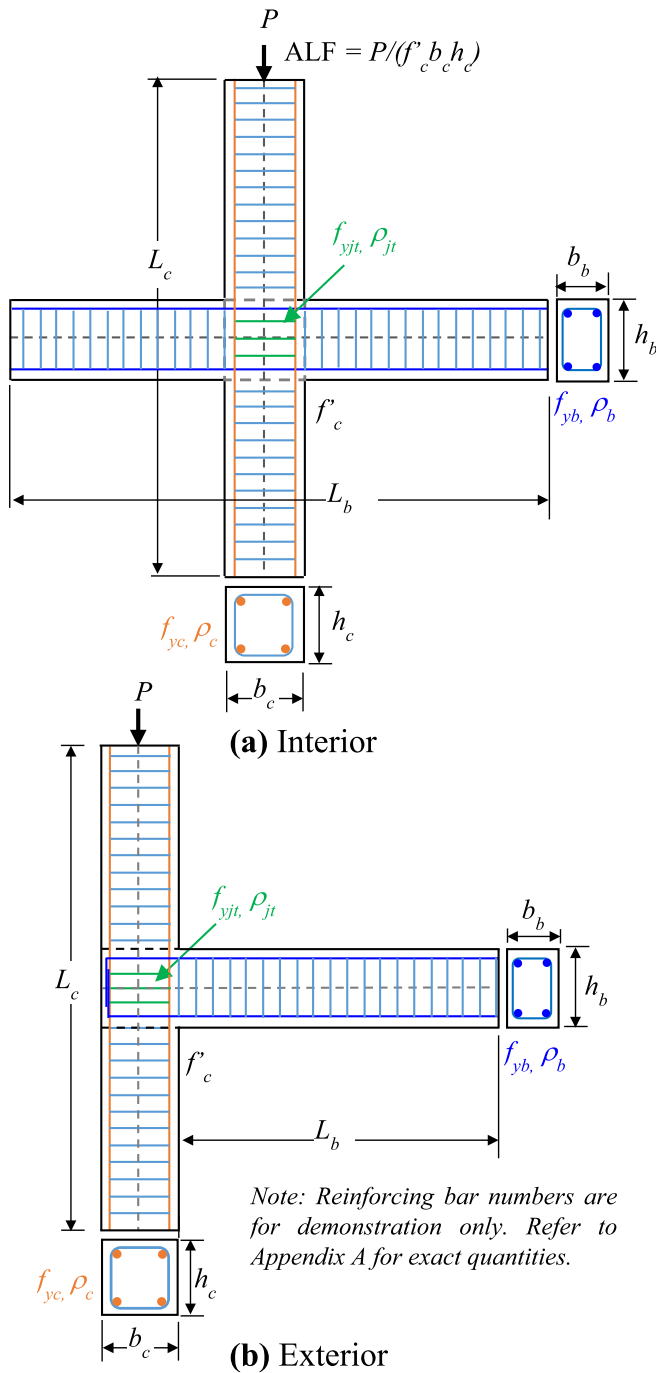


Fig. 5. Common properties of experimental specimens.

biases for  $t^{\text{th}}$  iterations, and  $S_{dw(t-1)}$  and  $S_{db(t-1)}$  represent  $S_d$  terms related to the weights and biases for  $(t-1)^{\text{th}}$  iterations.

With the goal of capturing the advantages of both stochastic momentum gradient descent and root mean square propagation, Adam is implemented in the proposed FFNN by using TensorFlow [37], which is an open-source machine learning platform in Python programming language [38].

A parametric study is conducted to determine the most efficient network configuration and the optimum number of iterations. The experimental database is split into training (80%), testing (10%), and validation (10%) datasets. The network with the components discussed above is trained, tested, and validated with these sets. The MSEs are computed for various network configurations and number of iterations.

Table 1

Observed failure modes in the experimental database.

Failure modes		S	S-F	B	Total
Exterior	w	116	93	2	211
	w/o	79	19	12	110
Interior	w	44	88	0	132
	w/o	23	25	0	47
Total		262	225	14	501

w/o: without and w: with transverse reinforcement.

As shown in Fig. 3a, the most efficient network configuration was found for a single hidden layer with 27 neurons. As shown in Fig. 3b, 100 iterations were found to give the lowest MSEs for the training, testing, and validation, and thus used in the developed network.

The final configuration of the network is presented in Fig. 4. The 13 input variables include the followings:  $f'_c$  is the concrete compressive strength;  $\rho_{jt}$  is the joint transverse reinforcement ratio;  $f_{yjt}$  is the joint transverse reinforcement yield strength;  $\rho_b$  is the beam longitudinal reinforcement ratio;  $f_{yb}$  is the beam longitudinal reinforcement yield strength;  $b_b$  is the beam width;  $h_b$  is the beam depth;  $\rho_c$  is the column longitudinal reinforcement ratio;  $f_{yc}$  is the column longitudinal reinforcement yield strength;  $b_c$  is the column width;  $h_c$  the column depth; ALF is the axial load factor which equals to  $P/f'_c h_c b_c$  where  $P$  is the axial load applied to the column, and JT is the joint type. The output variable is the joint shear strength,  $\tau_{pred}$ .

### 3.1. Experimental database

An experimental database of 598 reinforced concrete beam-column joint specimens is compiled from 153 previously published research studies and presented in Appendix A. The common properties of the specimens include: i) the top beam reinforcing bars are hooked 90 degrees toward the joint core for exterior joints and continuous for interior joints; ii) the bottom beam reinforcing bars are either embedded straight or hooked towards the joint core for exterior joints and continuous for interior joints; iii) the vertical column reinforcing bars passing the joint core are straight; and iv) the specimens are planar without out-of-plane elements. Fig. 5 illustrates the common reinforcing bar configuration of the specimens.

The experimental database includes 273 exterior joints with transverse reinforcement, 120 exterior joints without transverse reinforcement, 148 interior joints with transverse reinforcement, and 57 interior joints without transverse reinforcement. As presented in Table 1, the vast majority of specimens experienced a joint shear failure (S) or a combined joint shear and interface flexure failure (S-F). Only a few specimens experienced a bond slip failure (B) which is a failure mode predominantly experienced by joints with sub-standard longitudinal reinforcement detailing. 97 specimens with missing or unreported failure modes are not included in Table 1. More details on the complete experimental database are provided in Appendix A.

### 3.2. Exploratory data analysis (EDA)

An exploratory data analysis is performed to understand the characteristics of the database and detect and eliminate any outliers before using the database for the development of the identified network configuration in Fig. 4. The data structure of variables is defined as either continuous or categorical. The continuous variables include measurable values within a range while the categorical variables represent distinct groups or classes. Out of 14 variables (13 input and 1 output), only JT is a categorical variable which is converted into a numerical value: 0 for an interior joint, and 1 for an exterior joint.

The presence of outliers in the database can adversely affect any ANN, leading to overfitting or underfitting and reducing its accuracy. The Cook's distance method [39,40] is used to detect the outliers in the



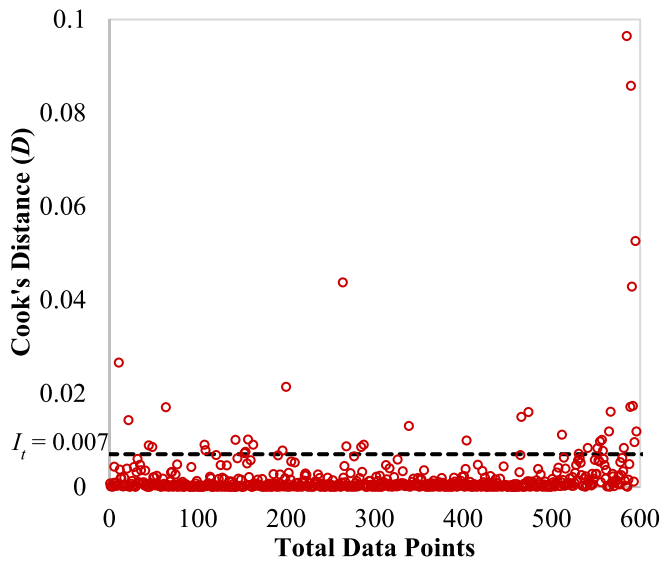


Fig. 6. Outlier detection using Cook's distance method.

Table 2  
Statistical description of the database after EDA.

Variable	Min	Max	Unit
Concrete compress. strength ( $f'_c$ )	15.8	102.0	MPa
Beam-column joint transverse reinforcement ratio, ( $\rho_{jt}$ )	0.0	2.6	%
Joint transverse reinforcement yield strength, ( $f_{yjt}$ )	235	1374	MPa
Beam rebar ratio ( $\rho_b$ )	0.4	4.3	%
Beam rebar yield strength ( $f_{yb}$ )	286	1091	MPa
Depth of beam ( $h_b$ )	150	750	mm
Width of beam ( $b_b$ )	100	610	mm
Column rebar ratio ( $\rho_c$ )	0.3	7.7	%
Column rebar yield strength ( $f_{yc}$ )	274	1092	MPa
Depth of column ( $h_c$ )	140	700	mm
Width of column ( $b_c$ )	100	900	mm
Axial load factor (ALF)	0.0	0.7	%
Joint type (JT)	0	1	
Shear Strength ( $\tau$ )	1.3	17.4	MPa

database. A data point is defined as an outlier if the computed Cook's distance ( $D_i$ ), in Eq. (10), exceeds the threshold limit ( $I_t$ ) in Eq. (11). In these equations,  $\tau_{pred}$  is the predicted shear strength,  $\tau_{pred(i)}$  is the predicted shear strength when a data point, say  $i^{th}$  point, is excluded from the database,  $p$  is the total number of weights and biases associated with a data point, MSE is the mean squared error as defined in Eq. (3), and  $n$  is the total number of data points in the database.

$$D_i = \frac{\sum_{i=1}^n (\tau_{pred} - \tau_{pred(i)})^2}{pMSE} \quad (10)$$

$$I_t = \frac{4}{n} \quad (11)$$

The results of the EDA for the entire database are presented in Fig. 6, where 43 data points are identified as outliers. These outliers are removed from the experimental database, leaving a resulting database with 555 data points.

Table 2 shows the ranges of parameter values for the resulting database, which covers a wide range to provide a general applicability for the developed network. It is important to note that neural networks are not appropriate for extrapolation of data. Therefore, they should only be used for the input inside the minimum and maximum data ranges of the parameters used in the training.

A correlation coefficient analysis is performed to quantify the correlation between the input and output variables using Eq. (12) where R

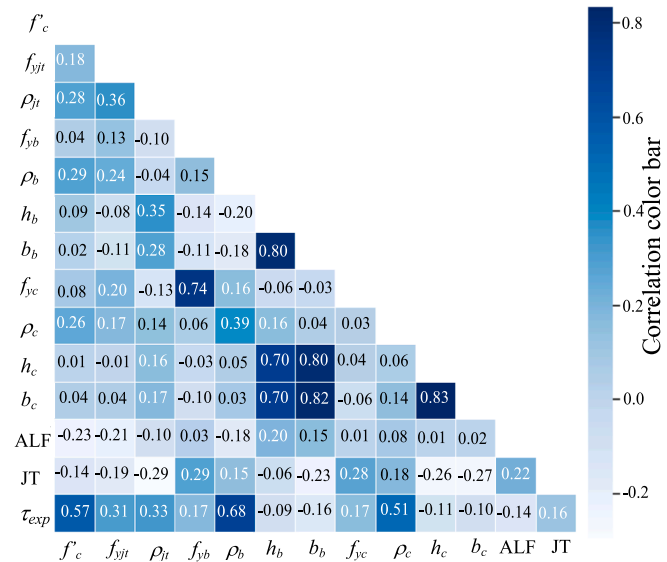


Fig. 7. Correlation coefficient matrix.

Table 3  
Data split for training, testing, and validation.

Joint type	Interior		Exterior		Total
	w/o	w	w/o	w	
Training (80 %)	43	107	91	204	445
Testing (10 %)	5	13	11	26	55
Validation (10 %)	5	13	11	26	55
Total	53	133	113	256	555

w/o: without and w: with transverse reinforcement.

is the correlation coefficient,  $n$  is the number of data points, and  $X$  and  $Y$  are any two variables for which the correlation is being calculated.

$$R = \frac{n \sum_{i=1}^n XY - (\sum_{i=1}^n X)(\sum_{i=1}^n Y)}{[n \sum_{i=1}^n X^2 - (\sum_{i=1}^n X)^2][n \sum_{i=1}^n Y^2 - (\sum_{i=1}^n Y)^2]} \quad (12)$$

The results of the correlation coefficient analysis are presented in Fig. 7 using a heatmap, which is a graphical representation of the correlation matrix. A correlation matrix may be used to summarize the data, as input for a more advanced investigation, or as a diagnostic tool for an advanced analysis [41,42]. The correlation coefficients range from +1 to -1, where +1 indicates the highest positive (direct) correlation and -1 indicates the highest negative (inverse) correlation. The shown heatmap uses a correlation color bar, from -0.2 to +0.8 as applicable to this study, where a darker color indicates a stronger correlation. For instance, the correlation coefficient between the input concrete compressive strength ( $f'_c$ ) and output shear strength ( $\tau_{exp}$ ) is 0.57, indicating a strong positive correlation of 57%. The darker color cells in the final row indicate the strong correlations between input and output variables.

### 3.3. Training, testing, and validation

Using 555 data points, which passed the EDA, and the final network configuration, the training, testing, and validation processes are repeated. A random sampling method is used to ensure all data has an equal chance of being selected [43] in a data split of 80%, 10%, and 10%, which is a common approach also used in other studies [28,44,45]. The distribution of specimen types is shown in Table 3.

The training of the network is carried out by performing 100 iterations, as found to give the lowest MSEs in Section 3, in which the forward and back propagations are applied to each input data point. The

**Table 4**  
Performance evaluation metrics.

Metrics	Formula
R	$\frac{n \sum \tau_{exp} \tau_{pred} - (\sum \tau_{exp})(\sum \tau_{pred})}{\sqrt{[n \sum \tau_{exp}^2 - (\sum \tau_{exp})^2] [n \sum \tau_{pred}^2 - (\sum \tau_{pred})^2]}}$ (13)
R <sup>2</sup>	$1 - \frac{\sum (\tau_{exp} - \tau_{pred})^2}{\sum (\tau_{exp} - \bar{\tau}_{exp})^2}$ (14)
MAE	$\frac{1}{n} \sum  \tau_{exp} - \tau_{pred} $ (15)
MSE	$\frac{1}{n} \sum (\tau_{exp} - \tau_{pred})^2$ (16)
RMSE	$\sqrt{\frac{1}{n_s} \sum (\tau_{exp} - \tau_{pred})^2}$ (17)
CV	$\frac{RMSE}{\frac{1}{n} \sum \tau_{pred}} \times 100$ (18)

iterations are completed once all data points have been used. At the end of each iteration, the calculation either continues to the next iteration or stops if the maximum number of iterations is reached. This includes the training process. Subsequent to the training process, the testing of the network is carried out by performing the forward propagation and computing the error for each input data point. The back propagation is not performed during the testing process. Because of this, the weights and biases are not updated, and multiple iterations are not performed.

The accuracy and reliability of the proposed network are evaluated using six performance evaluation metrics. Table 4 shows these metrics and their formulations. R is the correlation coefficient which is described previously in Section 3.2. It is used here to evaluate the correlation between the predicted and experimental shear strength values,  $\tau_{pred}$  and  $\tau_{exp}$ . R ranges from 0 to 1 where 1 indicates the highest correlation. R<sup>2</sup> is the determination coefficient which indicates the extent to which the predicted value matches the experimental value regardless of their direction. R<sup>2</sup> ranges from 0 to 1 where 1 indicates the best fit. MAE is the mean absolute error which is the average error between the predicted and experimental values. MSE is the mean squared error which is the average squared differences between predicted and experimental values. RMSE is the root mean squared error which is the average magnitude of the errors between predicted and experimental values. CV is the coefficient of variation which is the ratio of the standard deviation to the mean. For the error metrics (MAE, MSE, and RMSE) and CV, smaller numbers indicate more accurate results.

The scatterplots of the predicted-to-experimental shear strength ratios are shown in Fig. 8 for the training, testing, and validation processes. In these plots, an ideal result, where the network predicts exactly the experimental results, would be a 45° line ( $y = x$ ) with  $R^2 = 1$ , which is close to the graph obtained in the training process (Fig. 8a). The testing and validation were performed with the experimental data that was not used in the training (i.e., never seen by the network) as described above. As shown in Fig. 8b and 8c, the accuracy in the testing

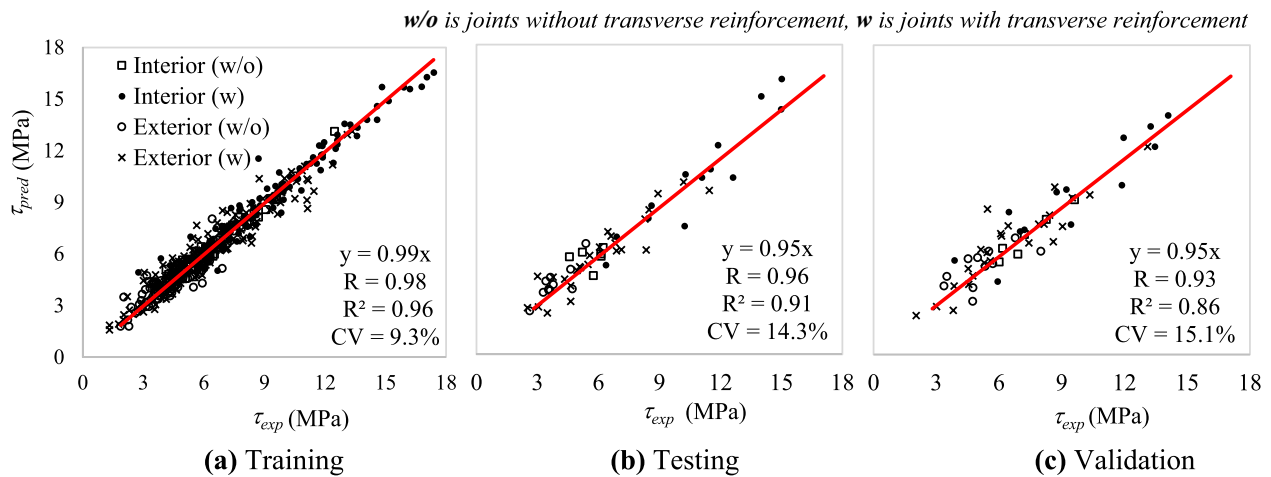


**Fig. 8.** Scatterplots of the predicted-to-experimental shear strength ratios.

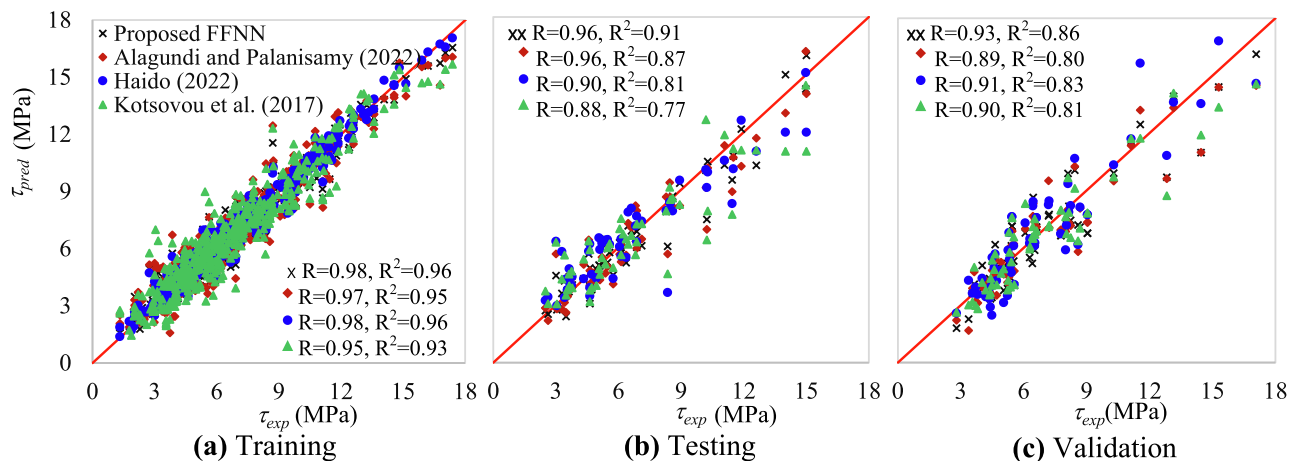


**Fig. 9.** Global performance comparison of the proposed network with three existing networks.

**Table 5**  
Error and coefficient of variation comparisons.

Network	MAE	MSE	RMSE	CV(%)
Proposed FFNN	0.72	0.92	0.95	14.7 %
Alagundi and Palanisamy (2022)	0.84	1.36	1.16	17.5 %
Haido (2022)	0.91	1.47	1.21	17.8 %
Kotsovou et al. (2017)	0.94	1.68	1.29	19.0 %

and validation is similar to that in the training with a larger coefficient of variation and a slightly less inclined trendline ( $y = 0.95x$  versus  $y = 0.99x$  from training). This indicates that the network predictions are slightly on the conservative side in favor of safety. The average predicted-to-experimental shear strength ratio for the 110 testing and validation specimens is 0.99, with a coefficient of variation of 14.7 %. These results show that the developed network is able to make accurate and reliable predictions of the joint shear strength for all four combinations of joint types.

**4. Comparisons with other networks from the literature**

To further investigate the accuracy, the proposed network is compared with three existing networks from literature, developed by Alagundi and Palanisamy [28], Haido [29], and Kotsovou et al. [24]. The comparisons use the same experimental database of 555 specimens and include: *i*) global performance evaluation metrics based on all joint types; *ii*) local performance evaluation metrics based on specific joint types; and *iii*) variable evaluation metrics with respect to the input variables.

Fig. 9 presents the global performance evaluation results for the training, testing, and validation datasets. In all three cases, the proposed network, denoted as FFNN, provides more accurate or same R and R<sup>2</sup> values. All four networks have diminished accuracies for the testing and validation datasets while the proposed FFNN still provides more accurate results. For instance, the R values for the proposed FFNN are 0.98 for the validation dataset as compared to 0.89, 0.91 and 0.90 for the three existing networks. With less than 10 % deviation from the experimental values, the accuracy obtained from the proposed FFNN is well within the margins of accuracy one could expect to achieve when modeling reinforced concrete joint failures [12,46,47].

Table 5 presents the performance evaluation metrics in terms of the errors and coefficient of variations for the testing and validation

processes including 110 data points. For all metrics, the proposed FFNN returns smaller errors and CV values indicating superior accuracy and reliability.

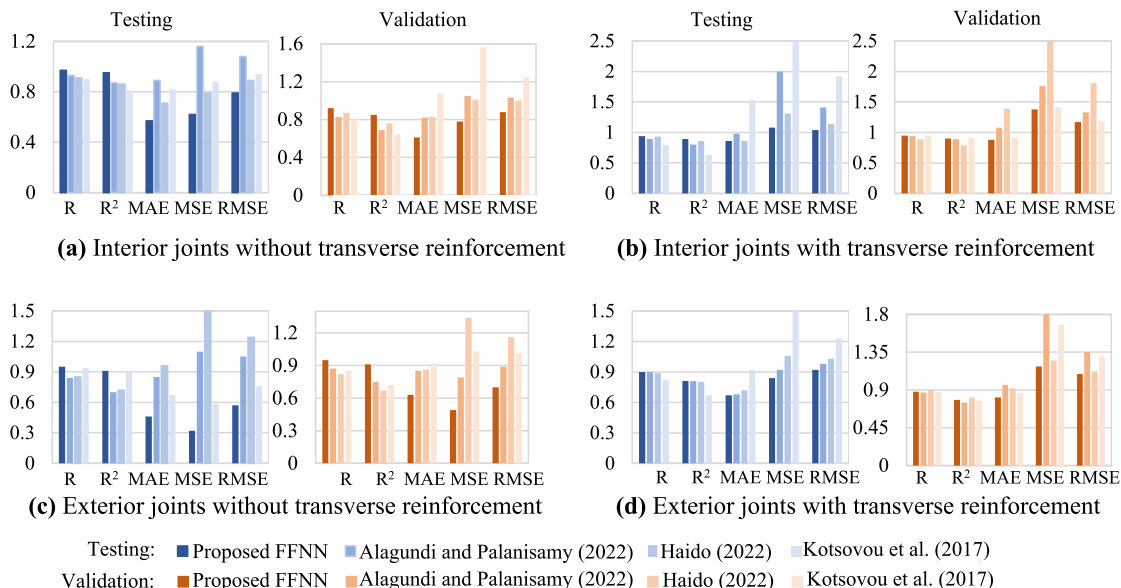
Fig. 10 presents the local performance evaluation metrics based on the joint types, including interior and exterior joints with or without transverse reinforcement, for the proposed network as compared to the three existing networks. The same testing and validation datasets were used including 55 data points each. For all types of joints, the proposed network yields higher values of R and R<sup>2</sup> and lower values of MAE, MSE, and RMSE indicating superior accuracy. For interior joints without transverse reinforcement (10 data points), the proposed network provides increased R and R<sup>2</sup> by an average of 9.4 % and 19.7 %, respectively, and reduced MAE, MSE, and RMSE by an average of 31.2 %, 33.3 %, and 18.7 %, respectively as compared to the three existing networks. For interior joints with transverse reinforcement (26 data points), R and R<sup>2</sup> are increased by 3.9 %, and 7.8 %, and MAE, MSE, and RMSE are lowered by an average of 21.1 %, 35.9 %, and 20.4 %, respectively. For exterior joints without transverse reinforcement (22 data points), R and R<sup>2</sup> are increased by 9.2 % and 16.7 % while MAE, MSE, and RMSE are reduced by 31.9 %, 67.6 %, and 43.7 %, respectively. For the exterior joints with transverse reinforcement (52 data points), R and R<sup>2</sup> are increased by 1.5 %, and 3.8 %, and MAE, MSE, and RMSE are reduced by 11.6 %, 24.3 %, and 13.1 %, respectively. These results clearly show the accuracy and reliability of the proposed network for all joint types considered. The improved accuracy for the joints with no transverse reinforcement, which are traditionally more challenging to capture using mechanics-based models, is particularly notable.

Table 6 compares the coefficient of variations obtained from the proposed network with the other networks for the testing and validation processes including 110 data points. The results indicate that the proposed network provides less variation for the predicted-to-experimental

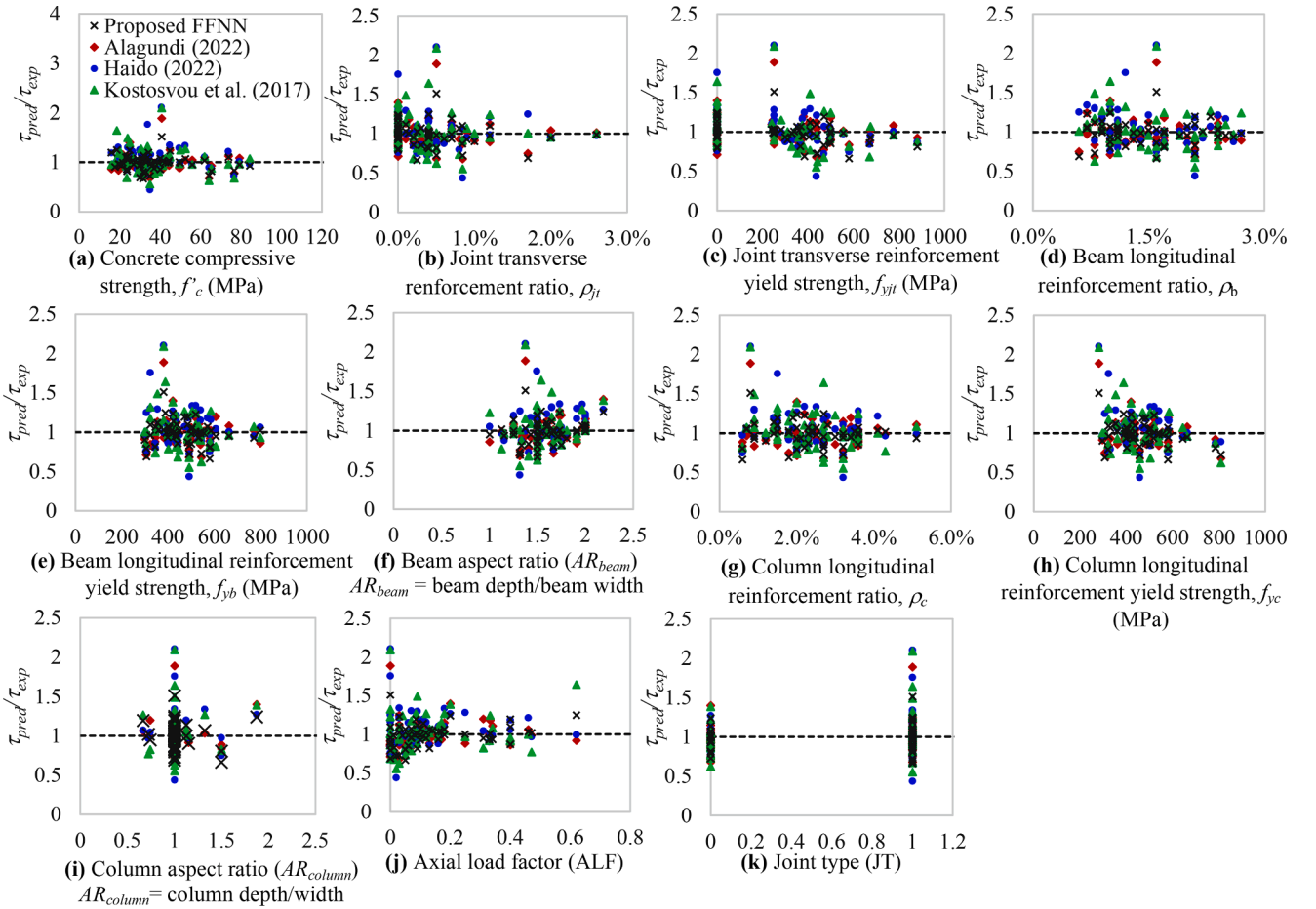
**Table 6**  
Coefficient of variation comparisons.

CV (%)	Interior		Exterior	
	w/o	w	w/o	w
Proposed FFNN	11.9 %	10.7 %	14.8 %	17.1 %
Alagundi and Palanisamy (2022)	13.7 %	12.5 %	19.7 %	20.5 %
Haido (2022)	13.9 %	14.6 %	26.9 %	17.5 %
Kotsovou et al. (2017)	17.5 %	13.2 %	21.3 %	21.2 %

w/o: without and w: with transverse reinforcement.



**Fig. 10.** Local performance comparison of the proposed network with three existing networks.



accuracy and reliability of the proposed network.

Fig. 11. Input variable range comparison of the proposed network with three existing networks.

shear strength ratios, and thus is more reliable.

As the final assessment, the predictive capabilities of the proposed network are compared to the networks from the literature with respect to the input variables. Fig. 11 presents the scatterplots of the predicted-to-experimental shear strength ratios across the complete ranges of each input variable. Beam and column width and depth variables are combined into two plots using aspect ratios. In these plots, the ideal ratio, where the network predictions are exactly equal to the experimental values, is shown with a horizontal line at 1.0. For all 13 input variables, the predictions of the proposed network are closer to the 1.0 line with less scatter and without a visible bias as compared to the other networks. These results further demonstrate the accuracy and reliability of the proposed network.

### 5. Derivation of joint spring curves

The lumped-plasticity approach is commonly used for the analysis of frames where plastic hinges are inserted at the critical locations of beams and columns with pre-defined hinge curves that represent the post-yield behavior in one or more degrees of freedom [48]. In these analyses, a rotational spring can be inserted at the intersection of beams and columns as a plastic hinge to define the post-yield behavior of joints. The proposed network is used to derive the shear stress–strain and moment-rotation curves to define the behavior of joint springs.

The rotational spring curves are derived, using the joint shear strength predicted by the proposed FFNN, based on four points: (1) cracking, (2) yielding, (3) maximum, and (4) residual. The cracking strength is defined as  $0.48\sqrt{f'_c}$  as recommended by Anderson et al. [45].

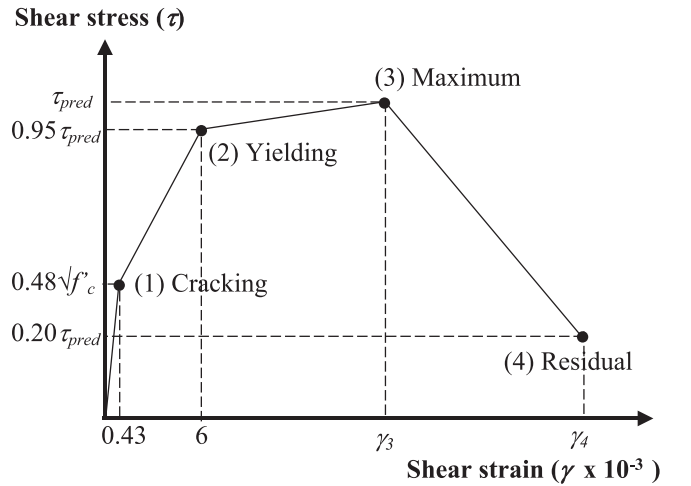


Fig. 12. Shear stress–strain curve.

The yield and residual strengths are 95 % and 20 % of the shear strength ( $\tau_{pred}$ ), respectively, adopted by Jeon [12] based on an experimental test result of 154 specimens. The shear strain values ( $\gamma$ ) corresponding to the cracking and yield strengths are adopted from Anderson et al. [49] based on the experimental test results of 11 specimens. The shear strains corresponding to the maximum and residual strengths are also based on the experimental test results of 154 specimens [12]. The resulting shear



**Table 7**  
Shear strain and rotation values ( $\times 10^{-3}$ ) for different types of joints.

Joint type	Interior		Exterior	
	w/o	w	w/o	w
$\gamma_1$ and $\theta_1$	0.43			
$\gamma_2$ and $\theta_2$	6			
$\gamma_3$ and $\theta_3$	19	20	16	20
$\gamma_4$ and $\theta_4$	117	187	77	185

w/o: without and w: with transverse reinforcement.

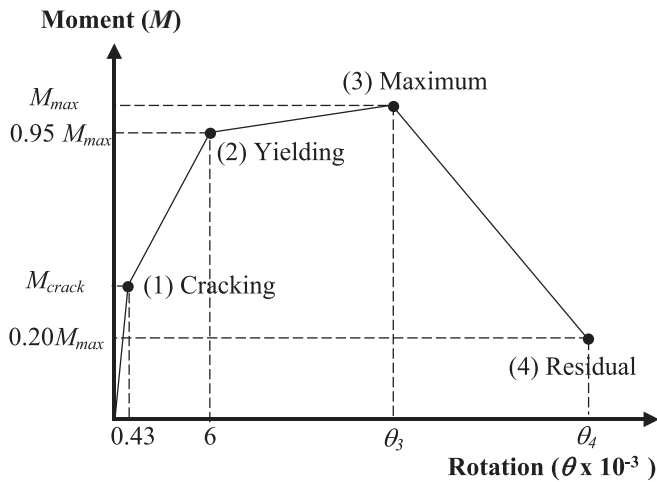


**Fig. 13.** Moment-rotation curves for the definition of a rotational spring.

stress-strain curve is presented in Fig. 12 with the shear strain ( $\gamma$ ) values summarized in Table 7 for different types of joints.

To define a rotational spring in a global frame analysis model, a moment-rotation curve is typically required. This curve is obtained by converting the shear stress-strain curve into an equivalent moment-rotation curve using Eqs. (19), (20) and (21) adopted from Celik and Ellingwood [50].

$$M_{max} = \tau_{pred} A_j \frac{1}{\frac{1-h_c/L_b}{jh_b} - \frac{1}{L_c}} \quad (19)$$

$$M_{crack} = (0.48 \sqrt{f'_c}) A_j \frac{1}{\frac{1-h_c/L_b}{jh_b} - \frac{1}{L_c}} \quad (20)$$

$$\theta = \gamma \quad (21)$$

$M_{max}$  is the equivalent moment capacity;  $M_{crack}$  is the equivalent cracking moment;  $h_b$  is the beam depth;  $h_c$  is the column depth;  $A_j$  is the joint core area ( $A_j = h_b \times h_c$ );  $L_c$  is the length of the column between the points of contraflexure;  $L_b$  is the length of beam between the points of contraflexure; and  $j$  is a constant taken as 0.875. Since the joint rotation is the change in the angle between the two edges of the joint core, the rotation is equivalent to the shear strain as stated in Eq. (21). The resulting moment-rotation curve is presented in Fig. 13 with the rotation values summarized in Table 7 for different types of joints. More details on this approach and application to various joint configurations, including the joints with straight reinforcing bar embedment, are provided in Suwal and Guner [11].

To facilitate the calculation process, a spreadsheet tool [51] is created and shared as a freeware for the use of engineers and researchers. A user bulletin [52] is also prepared to demonstrate the application and experimental validation of the spreadsheet with four specimens. The spreadsheet executes the proposed FFNN calculations and provides the shear strength ( $\tau_{pred}$ ) for a given beam-column joint configuration. The predicted strength is then converted to shear

stress-strain and moment-rotation curves using the approach defined above. The abscissa and ordinate values calculated in the spreadsheet can readily be used for the definition of joint hinges in common global frame analysis software.

## 6. Summary and conclusions

A feed-forward artificial neural network (FFNN) is developed to predict the shear strengths of reinforced concrete beam-column joints. A comprehensive database of 555 data points, which passed the exploratory data analysis, is used to train, test, and validate the proposed network for applicability to a wide range of input variables and joint configurations. The accuracy and reliability of the proposed network are evaluated using a comprehensive set of evaluation metrics. The proposed network is compared with three existing networks from the literature based on global, local, and input variable performance evaluation metrics. In addition, the proposed FFNN is used to derive the shear stress-strain and moment-rotation curves required for defining joint hinges in global frame analyses, and a spreadsheet tool is developed to execute the network formulations. The results of this study support the following conclusions:

1. Feed-forward artificial neural networks can be developed to predict the shear strengths of reinforced concrete beam-column joints accurately, reliably, and rapidly.
2. The datasets used in the training and testing of a neural network play a critical role in identifying the optimum parameters and network layout. An exploratory data analysis is recommended to understand the characteristics of the database and detect and eliminate any outliers before using the data for the development of a network.
3. The exploratory data analysis detected and eliminated 43 outliers from a database of 598 experimental specimens in this study. The use of the remaining database for the development of the proposed FFNN helped improve its accuracy and reliability.
4. The proposed FFNN is shown to predict the shear strengths of reinforced concrete beam-column joints rapidly and accurately. The predicted-to-experimental shear strength ratios for the 110 testing and validation specimens provided a mean of 0.99 and a coefficient of variation of 14.7 %.
5. The proposed FFNN is shown to provide more accurate and reliable response simulations than three existing networks from the literature. It provided a 4.3 % increase in the correlation coefficient and 8.7 % increase in the determination coefficient while providing a 18.7 % decrease in the coefficient of variation for the 110 experimental data points used in the testing and validation, as compared to the average values obtained from three existing networks.
6. The approach presented for deriving the shear stress-strain and moment-rotation curves enables the application of the proposed network in plastic-hinge-based frame analyses. The developed spreadsheet executes the required calculations and facilitates defining joint hinges in global frame analysis models.

## Declaration of Competing Interest

The authors declare that they have no known competing financial interests or personal relationships that could have appeared to influence the work reported in this paper.

## Data availability

Data will be made available on request.

## Appendix A. . Experimental database

The experimental database compiled for the development of the proposed FFNN is presented in Table A1.. It comprises 598 experimental

Table A1

Experimental database compiled for the development of the proposed FFNN.

No. of studies	S.N	Research Studies	Specimen	Joint Type	$f'_c$ (MPa)	$\rho_{jt}$	$f_{yjt}$ (MPa)	$\rho_b$	$f_{yb}$ (MPa)	$h_b$ (mm)	$b_b$ (mm)	$\rho_c$	$f_{yc}$ (MPa)	$h_c$ (mm)	$b_c$ (mm)	ALF	$\tau_{exp}$	Failure Mode
1	1	Adachi et al. (1995)	A0	Exterior	73.9	0.5 %	939	2.0 %	969	250	160	3.1 %	969	220	220	0.06	10.3	S
2	2	Alire (2002)	PEER0995	Interior	60.4	0.0 %	0	1.1 %	504	508	406	1.2 %	505	457	406	0.11	7.2	S-F
	3	Alire (2002)	PEER1595	Interior	61.5	0.0 %	0	0.9 %	841	508	406	3.5 %	538	457	406	0.11	10.5	S-F
	4	Alire (2002)	PEER4150	Interior	33.0	0.0 %	0	2.2 %	545	508	406	3.5 %	545	457	406	0.10	11.3	S-F
3	5	Almusallam and Al-Salloum (2007)	IC1	Interior	30.0	0.0 %	0	2.1 %	420	350	160	1.6 %	420	300	160	0.20	6.4	S-F
	6	Almusallam and Al-Salloum (2007)	IC2	Interior	25.0	0.0 %	0	2.1 %	420	350	160	1.6 %	420	300	160	0.20	4.6	S-F
4	7	Al-Salloum et al. (2011)	ECON1	Exterior	33.4	0.0 %	0	2.1 %	510	350	160	1.6 %	510	300	160	0.20	4.6	S
5	8	Alva et al. (2007)	LVP2	Exterior	44.2	0.3 %	602	2.7 %	594	400	200	3.3 %	594	300	200	0.15	7.3	S
	9	Alva et al. (2007)	LVP4	Exterior	24.6	0.3 %	602	2.7 %	594	400	200	3.3 %	594	300	200	0.15	5.5	S
	10	Alva et al. (2007)	LVP3	Exterior	23.9	0.6 %	602	2.7 %	594	400	200	3.3 %	594	300	200	0.15	6.1	S
	11	Alva et al. (2007)	LVP5	Exterior	25.9	0.6 %	602	2.7 %	594	400	200	3.3 %	594	300	200	0.15	6.4	S
6	12	Antonopoulos and Triantafillou (2003)	C1	Exterior	19.4	0.0 %	0	1.6 %	585	300	200	1.5 %	585	200	200	0.06	2.8	S
	13	Antonopoulos and Triantafillou (2003)	C2	Exterior	23.7	0.0 %	0	1.6 %	585	300	200	1.5 %	585	200	200	0.05	3.1	S
	14	Antonopoulos and Triantafillou (2003)	S-C	Exterior	30.6	0.0 %	0	1.6 %	585	300	200	1.5 %	585	200	200	0.12	3.6	S
7	15	Aoyama et al. (1993)	H2	Interior	45.6	0.5 %	441	0.8 %	544	300	200	2.7 %	544	300	300	0.04	7.0	S-F
	16	Aoyama et al. (1993)	H4	Interior	64.2	0.5 %	441	0.8 %	544	300	200	2.7 %	809	300	300	0.03	10.2	S-F
8	17	Atta et al. (2003)	G2-B	Exterior	60.0	0.0 %	0	1.1 %	360	400	200	2.4 %	360	200	200	0.17	5.8	S
	18	Atta et al. (2003)	G3-B	Exterior	62.0	0.3 %	240	1.1 %	360	400	200	2.4 %	360	200	200	0.16	5.6	S-F
	19	Atta et al. (2003)	G1-A	Exterior	67.0	0.5 %	240	1.1 %	360	400	200	2.4 %	360	200	200	0.15	5.6	J
	20	Atta et al. (2003)	G1-B	Exterior	36.0	0.5 %	240	1.1 %	360	400	200	2.4 %	360	200	200	0.28	5.8	J
	21	Atta et al. (2003)	G1-C	Exterior	33.0	0.5 %	240	1.1 %	360	400	200	2.4 %	360	200	200	0.30	5.7	J
	22	Atta et al. (2003)	G3-C	Exterior	68.0	0.5 %	240	1.1 %	360	400	200	2.4 %	360	200	200	0.15	5.6	S-F
	23	Atta et al. (2003)	G3-E	Exterior	68.0	0.5 %	240	1.1 %	360	400	200	2.4 %	360	200	200	0.15	5.5	S-F
	24	Atta et al. (2003)	G3-F	Exterior	62.0	0.5 %	240	1.1 %	360	400	200	2.4 %	360	200	200	0.16	5.3	Unknown
	25	Atta et al. (2003)	G2-C	Exterior	65.0	0.8 %	240	1.1 %	360	400	200	2.4 %	360	200	200	0.15	5.6	S-F
	26	Atta et al. (2003)	G3-D	Exterior	64.0	1.3 %	240	1.1 %	360	400	200	2.4 %	360	200	200	0.16	5.7	S-F
9	27	Beres et al. (1991)	E01	Exterior	26.1	0.0 %	0	0.8 %	490	610	356	2.0 %	517	406	406	0.13	2.9	B
	28	Beres et al. (1991)	E05	Exterior	31.5	0.0 %	0	0.8 %	490	610	356	2.0 %	519	406	406	0.24	3.3	B
	29	Beres et al. (1991)	E07	Exterior	29.3	0.0 %	0	0.8 %	490	610	356	2.0 %	519	406	406	0.12	2.8	B
	30	Beres et al. (1991)	E-10	Exterior	20.5	0.0 %	0	0.8 %	490	610	356	2.0 %	517	406	406	0.59	2.9	B
	31	Beres et al. (1991)	E-12	Exterior	18.9	0.0 %	0	0.8 %	474	610	356	0.9 %	499	406	406	0.14	2.2	B
	32	Beres et al. (1991)	E-13	Exterior	17.0	0.0 %	0	0.8 %	474	610	356	0.9 %	499	406	406	0.18	2.3	B
	33	Beres et al. (1991)	E04	Exterior	24.5	0.2 %	483	0.8 %	490	610	356	2.0 %	501	406	406	0.09	3.4	B
	34	Beres et al. (1991)	I-11	Interior	29.9	0.0 %	0	0.8 %	459	610	356	2.0 %	487	406	406	0.09	4.1	Unknown
	35	Beres et al. (1991)	I-13	Interior	25.0	0.0 %	0	0.8 %	341	610	356	2.0 %	550	406	406	0.10	4.4	Unknown
	36	Beres et al. (1991)	I-15	Interior	23.4	0.0 %	0	0.8 %	461	610	356	2.0 %	497	406	406	0.58	4.3	Unknown
	37	Beres et al. (1991)	I-17	Interior	21.2	0.0 %	0	0.8 %	472	610	356	0.9 %	472	406	406	0.17	3.5	Unknown
	38	Beres et al. (1991)	I-20	Interior	20.0	0.0 %	0	0.8 %	461	610	356	0.9 %	478	406	406	0.53	4.1	Unknown
10	39	Biddah (1997)	J4	Exterior	24.0	0.0 %	0	0.4 %	440	610	610	0.7 %	440	510	610	0.07	1.9	B
11	40	Chalioris (2008)	Jca-0	Exterior	20.6	0.0 %	0	1.2 %	470	300	200	1.2 %	470	300	200	0.10	1.7	S
	41	Chalioris (2008)	JA-0	Exterior	34.0	0.0 %	0	1.7 %	580	300	200	1.7 %	580	300	200	0.05	4.4	S
	42	Chalioris (2008)	Jcb-0	Exterior	23.0	0.0 %	0	1.7 %	470	300	200	1.2 %	470	300	200	0.10	2.0	S
	43	Chalioris (2008)	JB-0	Exterior	31.6	0.0 %	0	1.7 %	580	300	200	0.6 %	580	300	200	0.05	4.7	S
	44	Chalioris (2008)	Jca-s1	Exterior	21.0	0.2 %	470	1.2 %	470	300	200	1.2 %	470	300	200	0.10	1.3	S-F
	45	Chalioris (2008)	Jcb-s1	Exterior	23.0	0.2 %	470	1.7 %	470	300	200	1.2 %	470	300	200	0.10	2.0	S-F
	46	Chalioris (2008)	Jca-s2	Exterior	21.0	0.3 %	470	1.2 %	470	300	200	1.2 %	470	300	200	0.10	1.3	S
	47	Chalioris (2008)	Jca-s2	Exterior	23.0	0.3 %	470	1.7 %	470	300	200	1.2 %	470	300	200	0.10	2.0	S
	48	Chalioris (2008)	JB-s1	Exterior	32.0	0.2 %	580	1.7 %	580	300	200	1.7 %	580	300	200	0.05	4.6	Unknown

(continued on next page)

Table A1 (continued)

No. of studies	S.N	Research Studies	Specimen	Joint Type	$f'_c$ (MPa)	$\rho_{jt}$	$f_{jit}$ (MPa)	$\rho_b$	$f_{yb}$ (MPa)	$h_b$ (mm)	$b_b$ (mm)	$\rho_c$	$f_{jc}$ (MPa)	$h_c$ (mm)	$b_c$ (mm)	ALF	$\tau_{exp}$	Failure Mode
12	49	Chalioris (2008)	JA-s5	Exterior	34.0	0.8 %	580	1.7 %	580	300	200	1.7 %	580	300	200	0.05	4.5	Unknown
	50	Chang et al. (1997)	BCB1	Interior	54.7	0.0 %	0	1.3 %	354	400	300	2.3 %	354	500	300	0.18	6.4	S-F
	51	Chang et al. (1997)	BCS1	Interior	54.7	0.0 %	0	1.3 %	354	400	300	2.3 %	354	500	300	0.18	7.4	S-F
13	52	Chang et al. (1997)	BCS2	Interior	54.7	0.5 %	352	1.4 %	354	400	300	2.3 %	354	500	300	0.18	8.2	Unknown
	53	Chen (2006)	TDP2	Exterior	23.8	0.1 %	408	0.5 %	333	330	200	0.9 %	333	230	230	0.08	1.7	S
	54	Chen (2006)	TDP1	Exterior	22.9	0.1 %	408	0.5 %	348	330	200	0.9 %	348	230	230	0.09	1.8	S-F
14	55	Chen (2006)	TDD2	Exterior	24.0	0.1 %	408	0.8 %	354	330	200	0.9 %	354	230	230	0.09	2.5	S
	56	Chen and Chen (1999)	JC	Exterior	20.0	0.6 %	397	1.6 %	439	500	300	1.6 %	457	500	500	0.00	5.2	S-F
15	57	Chen and Chen (1999)	JE	Exterior	19.9	0.6 %	397	1.6 %	439	500	300	1.6 %	457	500	500	0.00	5.6	S-F
	58	Chutarat and Aboutaha (2003)	Specimen1	Exterior	27.6	1.2 %	365	1.4 %	483	500	356	2.8 %	483	406	406	0.00	5.6	S-F
16	59	Chutarat and Aboutaha (2003)	SpecimenA	Exterior	33.1	1.2 %	365	1.4 %	483	500	356	2.8 %	483	406	406	0.00	5.2	Unknown
	60	Clyde et al. (2000)	Unit 2	Exterior	46.2	0.0 %	0	2.4 %	746	406	305	2.2 %	742	457	305	0.10	7.5	S
	61	Clyde et al. (2000)	Unit 4	Exterior	41.0	0.0 %	0	2.4 %	746	406	305	2.2 %	742	457	305	0.25	7.1	S
	62	Clyde et al. (2000)	Unit 5	Exterior	37.0	0.0 %	0	2.4 %	746	406	305	2.2 %	742	457	305	0.25	6.8	S
17	63	Clyde et al. (2000)	Unit 6	Exterior	40.1	0.0 %	0	2.4 %	746	406	305	2.2 %	742	457	305	0.10	7.3	S
	64	Dehkordi (2019)	NS-70	Exterior	30.0	0.8 %	420	1.5 %	420	300	250	2.0 %	420	250	250	0.08	4.8	Unknown
	65	Dehkordi (2019)	RHS-70	Exterior	70.0	0.8 %	420	1.5 %	600	300	250	1.4 %	600	250	250	0.04	4.8	Unknown
18	66	Dehkordi (2019)	CNS-70	Exterior	30.0	0.8 %	420	1.8 %	600	300	250	1.4 %	420	250	250	0.08	7.4	Unknown
	67	Dhakal et al. (2005)	C1PD	Interior	31.6	0.0 %	0	2.7 %	538	550	300	2.2 %	538	500	350	0.11	7.7	S
19	68	Dhakal et al. (2005)	C1ND	Interior	31.6	0.0 %	0	2.7 %	538	550	300	2.2 %	538	500	350	0.11	8.9	S
	69	Dhakal et al. (2005)	C4ND	Interior	32.7	0.0 %	0	3.3 %	538	550	300	2.5 %	538	400	400	0.11	9.6	S
	70	Dhakal et al. (2005)	C1HD	Interior	31.6	0.0 %	0	2.7 %	538	550	300	2.2 %	538	500	350	0.11	8.7	S
	71	Dhakal et al. (2005)	C4HD	Interior	32.7	0.0 %	0	3.3 %	538	550	300	2.5 %	538	400	400	0.11	9.3	S
	72	Durrani and Wight (1985)	X1	Interior	34.3	0.8 %	352	1.5 %	345	419	279	3.1 %	414	362	362	0.05	7.2	S-F
	73	Durrani and Wight (1985)	X2	Interior	33.6	1.2 %	352	1.5 %	345	419	279	3.1 %	414	362	362	0.06	7.3	S-F
	74	Durrani and Wight (1985)	X3	Interior	31.0	0.8 %	352	1.1 %	345	419	279	2.0 %	331	362	362	0.05	5.4	S-F
20	75	Ehsani and Alameddine (1991)	LL8	Exterior	55.8	1.2 %	437	3.0 %	437	508	318	2.8 %	437	356	356	0.04	7.8	S-F
	76	Ehsani and Alameddine (1991)	LL14	Exterior	93.8	1.2 %	437	3.0 %	437	508	318	2.8 %	437	356	356	0.02	7.8	S-F
	77	Ehsani and Alameddine (1991)	LL11	Exterior	73.8	1.2 %	437	3.0 %	437	508	318	2.8 %	437	356	356	0.03	7.8	S
	78	Ehsani and Alameddine (1991)	HL8	Exterior	55.8	1.2 %	437	3.8 %	437	508	318	3.2 %	437	356	356	0.07	10	S
	79	Ehsani and Alameddine (1991)	HL11	Exterior	73.8	1.2 %	437	3.8 %	437	508	318	3.2 %	437	356	356	0.06	9.9	S
	80	Ehsani and Alameddine (1991)	HL14	Exterior	93.8	1.2 %	437	3.8 %	437	508	318	3.2 %	437	356	356	0.04	9.9	S
	81	Ehsani and Alameddine (1991)	LH11	Exterior	73.8	2.0 %	437	3.0 %	437	508	318	2.8 %	437	356	356	0.03	7.8	S-F
	82	Ehsani and Alameddine (1991)	LH14	Exterior	93.8	2.0 %	437	3.0 %	437	508	318	2.8 %	437	356	356	0.02	7.8	S-F
	83	Ehsani and Alameddine (1991)	LH8	Exterior	55.8	2.0 %	437	3.0 %	437	508	318	2.8 %	437	356	356	0.04	7.8	S-F
	84	Ehsani and Alameddine (1991)	HH8	Exterior	55.8	2.0 %	437	3.8 %	437	508	318	3.2 %	437	356	356	0.07	10	S-F
	85	Ehsani and Alameddine (1991)	HH11	Exterior	73.8	2.0 %	437	3.8 %	437	508	318	3.2 %	437	356	356	0.06	9.9	S-F
	86	Ehsani and Alameddine (1991)	HH14	Exterior	93.8	2.0 %	437	3.8 %	437	508	318	3.2 %	437	356	356	0.04	8.6	S-F
21	87	Ehsani et al. (1987)	4	Exterior	67.3	1.5 %	437	1.5 %	448	439	259	4.0 %	448	300	300	0.05	8.7	S-F
	88	Ehsani et al. (1987)	5	Exterior	44.6	1.5 %	437	1.7 %	448	439	259	2.5 %	448	300	300	0.06	6.9	S-F

(continued on next page)

Table A1 (continued)

No. of studies	S.N	Research Studies	Specimen	Joint Type	$f'_c$ (MPa)	$\rho_{jt}$	$f_{jit}$ (MPa)	$\rho_b$	$f_{yb}$ (MPa)	$h_b$ (mm)	$b_b$ (mm)	$\rho_c$	$f_{jc}$ (MPa)	$h_c$ (mm)	$b_c$ (mm)	ALF	$\tau_{exp}$	Failure Mode
	89	Ehsani et al. (1987)	1	Exterior	64.7	1.9 %	437	1.0 %	448	439	259	3.2 %	448	300	300	0.02	5.0	S-F
	90	Ehsani et al. (1987)	2	Exterior	67.3	1.9 %	437	1.2 %	448	439	259	3.2 %	448	300	300	0.06	6.1	S-F
	91	Ehsani et al. (1987)	3	Exterior	64.7	1.9 %	437	1.2 %	448	439	259	3.2 %	448	300	300	0.07	7.0	S-F
22	92	El-Amoury (2004)	T-S1	Exterior	30.8	0.0 %	0	1.3 %	477	400	250	1.3 %	477	400	250	0.19	5.5	S-F
	93	El-Amoury (2004)	T-SB3	Exterior	30.6	0.0 %	0	1.3 %	477	400	250	1.3 %	477	400	250	0.20	4.0	B
23	94	Endoh et al. (1991)	LA1	Interior	34.8	0.7 %	286	2.0 %	801	300	200	3.5 %	550	300	300	0.06	9.8	S
	95	Endoh et al. (1991)	HLC	Interior	40.6	0.4 %	290	1.7 %	368	300	200	2.7 %	360	300	300	0.05	8.4	S-F
	96	Endoh et al. (1991)	A1	Interior	30.6	0.6 %	320	2.0 %	780	300	200	3.5 %	539	300	300	0.06	9.2	S
24	97	Eshani and Wight (1985)	6B	Exterior	38.4	1.0 %	437	1.6 %	331	480	300	2.0 %	490	340	340	0.07	4.6	S-F
	98	Eshani and Wight (1985)	5B	Exterior	24.3	1.2 %	437	1.8 %	331	480	300	4.4 %	414	340	340	0.13	6.2	S
	99	Eshani and Wight (1985)	1B	Exterior	33.6	1.3 %	437	1.8 %	331	480	259	2.5 %	490	300	300	0.06	6.8	S
	100	Eshani and Wight (1985)	2B	Exterior	35.0	1.5 %	437	2.0 %	331	439	259	3.2 %	490	300	300	0.07	7.0	S
	101	Eshani and Wight (1985)	3B	Exterior	40.9	1.7 %	437	1.8 %	331	480	259	2.5 %	490	300	300	0.06	6.8	S
	102	Eshani and Wight (1985)	4B	Exterior	44.6	1.7 %	437	2.0 %	331	439	259	3.2 %	490	300	300	0.06	6.8	S-F
25	103	Faleschini et al. (2018)	1	Exterior	39.0	2.6 %	555	1.7 %	555	500	300	2.3 %	555	300	300	0.11	8.2	Unknown
	104	Faleschini et al. (2018)	2	Exterior	48.5	2.6 %	555	1.7 %	555	500	300	2.3 %	555	300	300	0.10	8.7	Unknown
	105	Faleschini et al. (2018)	3	Exterior	44.0	2.6 %	555	1.7 %	555	500	300	2.3 %	555	300	300	0.10	8.5	Unknown
26	106	Filiatrault et al. (1994)	Sp-1	Exterior	34.0	0.0 %	0	1.0 %	475	450	350	2.3 %	475	350	350	0.08	5.8	B
27	107	Fuji and Morita (1991)	B2	Exterior	30.0	0.5 %	291	1.6 %	409	250	160	3.1 %	387	220	220	0.07	5.1	S
	108	Fuji and Morita (1991)	B1	Exterior	30.0	0.5 %	291	1.7 %	1069	250	160	3.1 %	387	220	220	0.07	5.9	S
	109	Fuji and Morita (1991)	B3	Exterior	30.0	0.5 %	291	1.7 %	1069	250	160	3.1 %	387	220	220	0.24	6.6	S
	110	Fuji and Morita (1991)	B4	Exterior	30.0	1.5 %	291	1.7 %	1069	250	160	3.1 %	387	220	220	0.24	6.9	S
	111	Fujii and Morita (1987)	OBO	Interior	43.5	0.4 %	367	1.1 %	369	250	160	3.1 %	369	220	220	0.05	7.0	S-F
	112	Fujii and Morita (1991)	A1	Interior	40.2	0.5 %	291	1.7 %	1069	250	160	4.2 %	643	220	220	0.08	9.9	S
28	113	Fujii and Morita (1991)	A2	Interior	40.2	0.5 %	291	1.6 %	409	250	160	4.2 %	387	220	220	0.08	9.1	S
	114	Fujii and Morita (1991)	A3	Interior	40.2	0.5 %	291	1.7 %	1069	250	160	4.2 %	643	220	220	0.23	9.9	S
	115	Fujii and Morita (1991)	A4	Interior	40.2	1.5 %	291	1.7 %	1069	250	160	4.2 %	643	220	220	0.23	10.1	S
29	116	Ghobarah and Said (2002)	T1	Exterior	30.8	0.0 %	0	1.3 %	425	400	250	2.2 %	425	400	250	0.19	5.6	S-F
30	117	Goto and Joh (1996)	J-OH	Interior	31.5	0.0 %	0	2.4 %	538	350	200	3.8 %	578	300	300	0.28	9.6	S
	118	Goto and Joh (1996)	BJ-PL	Interior	29.7	0.4 %	326	1.4 %	395	350	200	3.1 %	640	300	300	0.17	6.5	S-F
	119	Goto and Joh (1996)	BJ-PH	Interior	30.5	0.9 %	326	1.4 %	395	350	200	3.1 %	640	300	300	0.17	6.9	S-F
	120	Goto and Joh (1996)	J-LO	Interior	24.0	0.3 %	355	1.8 %	697	350	200	2.0 %	388	300	450	0.17	8.4	S
	121	Goto and Joh (1996)	C5-LO	Interior	32.7	0.0 %	360	2.4 %	426	350	200	3.8 %	578	200	450	0.27	10.4	Unknown
	122	Goto and Joh (1996)	J-HH	Interior	32.8	1.6 %	381	2.4 %	426	350	200	3.8 %	578	300	300	0.27	9.6	S
	123	Goto and Joh (1996)	J-HO	Interior	31.4	1.6 %	381	2.4 %	426	350	200	3.8 %	578	300	300	0.28	9.3	S
	124	Goto and Joh (1996)	J-MM	Interior	32.4	0.8 %	381	2.4 %	426	350	200	3.8 %	578	300	300	0.27	9.7	S
	125	Goto and Joh (1996)	J-MO	Interior	32.7	0.8 %	381	2.4 %	426	350	200	3.8 %	578	300	300	0.27	10.0	S
31	126	Ha (1992)	1	Exterior	41.2	0.2 %	387	2.9 %	414	200	150	2.9 %	414	200	200	0.03	5.6	S-F
	127	Ha (1992)	4	Exterior	68.6	0.2 %	387	2.9 %	414	200	150	2.9 %	414	200	200	0.02	5.4	S-F
32	128	Hakuto et al. (2000)	O4	Interior	52.9	0.0 %	0	1.4 %	308	500	300	1.7 %	321	460	460	0.00	5.5	S-F
	129	Hakuto et al. (2000)	O5	Interior	32.8	0.0 %	0	1.2 %	306	500	300	1.7 %	321	460	460	0.00	5.8	S-F
33	130	Hamil (2000)	C7LN0	Exterior	38.4	0.0 %	0	1.4 %	500	300	110	3.6 %	500	150	150	0.05	5.9	S
	131	Hamil (2000)	C9LN0	Exterior	40.8	0.0 %	0	1.4 %	500	300	110	3.6 %	500	150	150	0.05	5.5	S
	132	Hamil (2000)	C4ALN0	Exterior	42.4	0.0 %	0	2.1 %	500	210	110	3.6 %	500	150	150	0.05	7.3	S
	133	Hamil (2000)	C6ALH0	Exterior	100.8	0.0 %	0	2.1 %	500	210	110	3.6 %	500	150	150	0.04	9.5	S
	134	Hamil (2000)	C6LN0	Exterior	51.2	0.0 %	0	2.1 %	500	210	110	3.6 %	500	150	150	0.04	6.4	S
	135	Hamil (2000)	C6LN1A	Exterior	48.8	0.0 %	0	2.1 %	500	210	110	3.6 %	500	150	150	0.05	7.5	S
	136	Hamil (2000)	C6LN1AE	Exterior	44.0	0.0 %	0	2.1 %	500	210	110	3.6 %	500	150	150	0.06	8.0	S
	137	Hamil (2000)	C7LN1	Exterior	37.6	0.3 %	500	1.4 %	500	300	110	3.6 %	500	150	150	0.06	6.6	S
	138	Hamil (2000)	C7LN3	Exterior	40.0	0.3 %	500	1.4 %	500	300	110	3.6 %	500	150	150	0.06	7.1	S
	139	Hamil (2000)	C9LN1	Exterior	38.4	0.3 %	500	1.4 %	500	300	110	3.6 %	500	150	150	0.06	5.5	S
	140	Hamil (2000)	C9LN3	Exterior	36.8	0.3 %	500	1.4 %	500	300	110	3.6 %	500	150	150	0.06	6.3	S
	141	Hamil (2000)	C6LN1R	Exterior	48.8	0.4 %	500	2.1 %	500	210	110	3.6 %	500	150	150	0.06	7.6	S
	142	Hamil (2000)	C4ALN1	Exterior	45.6	0.4 %	500	4.1 %	500	210	110	3.6 %	500	150	150	0.05	9.4	Unknown

(continued on next page)



Table A1 (continued)

No. of studies	S.N	Research Studies	Specimen	Joint Type	$f'_c$ (MPa)	$\rho_{jt}$	$f_{jit}$ (MPa)	$\rho_b$	$f_{yb}$ (MPa)	$h_b$ (mm)	$b_b$ (mm)	$\rho_c$	$f_{yc}$ (MPa)	$h_c$ (mm)	$b_c$ (mm)	ALF	$\tau_{exp}$	Failure Mode
	143	Hamil (2000)	C4ALN3	Exterior	52.0	0.6 %	500	4.1 %	500	210	110	3.6 %	500	150	150	0.04	11.2	Unknown
	144	Hamil (2000)	C4ALN5	Exterior	63.0	1.2 %	500	4.1 %	500	210	110	3.6 %	500	150	150	0.04	12.4	Unknown
	145	Hamil (2000)	C6LN3	Exterior	61.0	0.6 %	500	4.1 %	500	210	110	3.6 %	500	150	150	0.04	8.7	Unknown
	146	Hamil (2000)	C6LN5	Exterior	46.0	1.2 %	500	4.1 %	500	210	110	3.6 %	500	150	150	0.05	11.0	Unknown
	147	Hamil (2000)	C6ALH3	Exterior	121.0	0.6 %	500	4.1 %	500	210	110	3.6 %	500	150	150	0.04	12.2	Unknown
	148	Hamil (2000)	C7LN5	Exterior	50.0	1.2 %	500	2.7 %	500	300	110	3.6 %	500	150	150	0.04	10.2	Unknown
	149	Hamil (2000)	C9LN5	Exterior	44.0	1.2 %	500	2.7 %	500	300	110	3.6 %	500	150	150	0.05	8.7	Unknown
34	150	Hanson and Connor (1967)	V	Exterior	22.8	0.0 %	0	1.9 %	352	508	305	5.5 %	447	381	381	0.52	4.7	S
35	151	Hayashi et al. (1993)	NO47	Interior	54.2	0.7 %	347	1.7 %	382	400	300	2.2 %	645	400	400	0.20	7.6	S-F
	152	Hayashi et al. (1993)	NO48	Interior	54.2	0.7 %	347	1.1 %	645	400	300	2.2 %	645	400	400	0.20	8.5	S-F
	153	Hayashi et al. (1993)	NO49	Interior	54.2	0.7 %	347	1.9 %	599	400	300	2.2 %	645	400	400	0.20	11.9	S-F
	154	Hayashi et al. (1993)	NO50	Interior	54.2	0.7 %	347	0.8 %	858	400	300	2.2 %	645	400	400	0.20	8.4	S-F
36	155	Hiramatsu et al. (1995)	S1	Interior	52.2	0.3 %	876	1.5 %	836	300	210	2.3 %	836	300	300	0.20	11.7	S
37	156	Ho and Cho (2008)	NJC	Exterior	29.6	2.1 %	455	2.9 %	455	200	150	2.8 %	403	200	200	0.15	5.2	Unknown
	157	Ho and Cho (2008)	HJC	Exterior	49.5	2.1 %	455	2.9 %	455	200	150	2.8 %	403	200	200	0.15	5.0	Unknown
38	158	Hoffschild et al. (1995)	RCBC1	Exterior	26.3	0.0 %	0	1.2 %	566	200	165	1.3 %	566	190	190	0.10	4.5	S
39	159	Hwang (2004)	28-0 T0	Exterior	33.0	0.0 %	0	2.1 %	491	500	380	3.2 %	458	550	550	0.02	7.3	Unknown
	160	Hwang (2004)	28-3 T4	Exterior	35.0	0.8 %	436	2.1 %	491	500	380	3.2 %	458	550	550	0.02	8.4	Unknown
	161	Hwang (2004)	70-3 T44	Exterior	75.2	1.1 %	436	2.1 %	491	450	320	3.2 %	458	450	450	0.01	10.9	Unknown
	162	Hwang (2004)	70-1 T55	Exterior	69.7	0.3 %	469	2.1 %	491	450	320	3.2 %	458	450	450	0.01	11.1	Unknown
	163	Hwang (2004)	70-2 T5	Exterior	76.6	0.4 %	469	2.1 %	491	450	320	3.2 %	458	450	450	0.01	11.5	Unknown
	164	Hwang (2004)	70-3 T44	Exterior	76.8	1.1 %	498	2.1 %	491	450	320	3.6 %	458	420	420	0.01	10.5	Unknown
40	165	Hwang et al. (2005)	3 T3	Exterior	69.0	0.9 %	0	2.8 %	430	450	320	3.7 %	421	420	420	0.02	7.2	S-F
	166	Hwang et al. (2005)	2 T4	Exterior	71.0	0.9 %	0	2.8 %	430	450	320	3.7 %	421	420	420	0.02	6.9	S-F
	167	Hwang et al. (2005)	1 T44	Exterior	72.8	0.9 %	0	2.8 %	430	450	320	3.7 %	421	420	420	0.02	5.1	S-F
	168	Hwang et al. (2005)	3 T44	Exterior	76.8	0.9 %	0	2.8 %	430	450	320	3.7 %	421	420	420	0.01	5.0	Unknown
	169	Hwang et al. (2005)	0 T0	Exterior	67.3	0.0 %	0	1.6 %	430	450	320	3.7 %	421	420	420	0.02	6.4	S-F
	170	Hwang et al. (2005)	1B8	Exterior	61.8	0.0 %	0	1.6 %	435	450	320	3.7 %	430	420	420	0.02	8.0	S-F
	171	Hwang et al. (2005)	3 T4	Exterior	75.2	0.8 %	436	2.8 %	430	450	320	3.2 %	458	450	450	0.01	5.1	Unknown
	172	Hwang et al. (2005)	2 T5	Exterior	76.6	0.8 %	469	2.8 %	491	450	320	3.2 %	458	450	450	0.01	5.1	Unknown
	173	Hwang et al. (2005)	1 T55	Exterior	69.7	0.8 %	469	2.8 %	491	450	320	3.2 %	458	450	450	0.01	5.1	Unknown
	174	Hwang et al. (2005)	1 T44	Exterior	72.8	0.4 %	498	1.6 %	430	450	320	3.7 %	421	420	420	0.02	6.7	Unknown
41	175	Ilki et al. (2011)	JOP	Exterior	8.3	0.0 %	0	0.7 %	333	500	250	1.3 %	333	500	250	0.13	1.2	S
42	176	Inoue et al. (1990)	SP2	Interior	43.3	0.3 %	1253	1.8 %	473	417	301	1.8 %	473	440	440	0.28	10.3	S-F
	177	Ishida et al. (1996)	No. 1	Interior	25.8	0.8 %	354	1.3 %	383	550	300	1.2 %	378	500	500	0.11	6.3	S-F
43	178	Ishida et al. (2001)	CN	Interior	33.4	0.2 %	365	1.4 %	462	750	450	1.6 %	464	700	800	0.09	6.9	S-F
44	179	Ishida et al. (2004)	HS-HS	Interior	70.0	0.4 %	1116	1.1 %	707	300	200	1.8 %	707	300	300	0.10	12.6	S-F
	180	Ishida et al. (2005)	A-0	Exterior	27.0	0.5 %	271	1.5 %	700	250	160	3.1 %	700	220	220	0.15	5.4	S
	181	Ishida et al. (2005)	A-0-F	Exterior	27.0	0.5 %	271	1.5 %	467	250	160	3.1 %	467	220	220	0.15	5.2	S-F
45	182	Ishikawa and Kamimura (1990)	No. 3	Interior	23.3	1.0 %	330	1.6 %	373	250	180	3.2 %	373	250	250	0.18	7.3	Unknown
46	183	Iwaoka et al. (2005)	J15-3	Exterior	180.0	0.2 %	935	3.6 %	682	400	260	2.7 %	690	380	330	0.05	14.9	Unknown
	184	Iwaoka et al. (2005)	J10-1	Exterior	115.0	0.2 %	935	3.6 %	682	400	260	2.7 %	690	380	330	0.05	13.6	S
	185	Iwaoka et al. (2005)	J15-1	Interior	182.0	0.2 %	935	3.7 %	682	400	220	3.0 %	690	380	300	0.25	24.5	Unknown
47	186	Jinno et al. (1985)	NO05	Exterior	32.0	0.0 %	0	1.3 %	392	380	260	3.8 %	371.0	300	300	0.00	4.1	S
	187	Jinno et al. (1985)	NO06	Exterior	28.9	0.4 %	304	1.3 %	392	380	260	3.8 %	371	300	300	0.00	4.2	S-F
	188	Jinno et al. (1985)	NO07	Exterior	28.9	0.4 %	304	1.3 %	392	380	260	3.8 %	371	300	300	0.00	4.2	S-F
	189	Jinno et al. (1985)	NO08	Exterior	28.9	0.8 %	304	1.3 %	392	380	260	3.8 %	371	300	300	0.00	4.3	S-F
	190	Jinno et al. (1985)	NO09	Exterior	28.9	0.8 %	304	1.3 %	392	380	260	3.8 %	371	300	300	0.00	4.3	S-F
	191	Jinno et al. (1985)	NO10	Exterior	28.9	0.8 %	304	1.3 %	392	380	260	3.8 %	371	300	300	0.00	4.6	S-F
48	192	Jinno et al. (1991)	NO1	Interior	28.3	0.3 %	686	1.7 %	405	400	300	2.9 %	405	400	400	0.17	7.8	S-F
	193	Jinno et al. (1991)	NO2	Interior	28.3	0.3 %	686	1.7 %	913	400	300	2.9 %	913	400	400	0.17	9.4	S
	194	Jinno et al. (1991)	NO3	Interior	80.2	0.3 %	686	1.7 %	593	400	300	2.9 %	593	400	400	0.17	13.1	S-F
	195	Jinno et al. (1991)	NO4	Interior	80.2	0.3 %	686	1.7 %	593	400	300	2.9 %	593	400	400	0.17	14.6	S-F

(continued on next page)

Table A1 (continued)

No. of studies	S.N	Research Studies	Specimen	Joint Type	$f'_c$ (MPa)	$\rho_{jt}$	$f_{jit}$ (MPa)	$\rho_b$	$f_{yb}$ (MPa)	$h_b$ (mm)	$b_b$ (mm)	$\rho_c$	$f_{yc}$ (MPa)	$h_c$ (mm)	$b_c$ (mm)	ALF	$\tau_{exp}$	Failure Mode	
49	196	Jinno et al. (1991)	NO5	Interior	80.2	0.3 %	686	1.7 %	913	400	300	2.9 %	913	400	400	0.17	17.5	S-F	
	197	Jinno et al. (1991)	NO6	Interior	101.9	0.3 %	686	1.7 %	726	400	300	2.9 %	726	400	400	0.17	15.9	S-F	
	198	Jinno et al. (1991)	NO7	Interior	101.9	0.3 %	686	1.7 %	913	400	300	2.9 %	913	400	400	0.17	17.4	S-F	
	199	Jinno et al. (1991)	NO8	Interior	101.9	0.3 %	686	2.3 %	913	400	300	2.9 %	913	400	400	0.17	20.1	S-F	
	200	Joh and Goto (2000)	PL-13	Interior	26.4	0.4 %	366	1.0 %	363	350	200	2.2 %	402	300	300	0.09	6.0	S-F	
	201	Joh and Goto (2000)	PH-16	Interior	23.6	0.5 %	366	1.2 %	344	350	200	2.7 %	402	300	300	0.13	6.4	S-F	
	202	Joh and Goto (2000)	PH-13	Interior	26.3	0.5 %	366	1.4 %	363	350	200	2.7 %	402	300	300	0.13	7.3	S-F	
50	203	Joh and Goto (2000)	PH-10	Interior	25.6	0.5 %	366	1.2 %	372	350	200	2.7 %	402	300	300	0.11	7.0	S-F	
	204	Joh et al. (1988)	X0-1	Interior	21.3	0.2 %	363	0.8 %	363	350	150	1.1 %	363	300	300	0.16	4.2	Unknown	
51	205	Joh et al. (1989)	LO-NO	Exterior	27.9	0.1 %	380	2.4 %	606	350	200	2.5 %	581	260	350	0.02	4.8	S	
	206	Joh et al. (1989)	HO-NO	Exterior	29.6	0.4 %	380	2.4 %	606	350	200	2.5 %	581	260	350	0.02	6.3	S	
52	207	Joh et al. (1989)	MM-NO	Exterior	27.8	0.4 %	380	2.4 %	606	350	200	2.8 %	581	260	350	0.02	6.1	S	
	208	Joh et al. (1989)	HH-NO	Exterior	29.3	0.4 %	380	2.4 %	606	350	200	2.5 %	581	260	350	0.02	7.2	S	
	209	Joh et al. (1989)	H'O-NO	Exterior	31.5	0.4 %	380	2.4 %	606	350	200	2.5 %	581	260	350	0.02	5.9	S	
	210	Joh et al. (1989)	LO-N96	Exterior	31.5	0.2 %	380	2.4 %	606	350	200	3.4 %	581	260	350	0.30	5.8	S	
	211	Joh et al. (1989)	HH-N96	Exterior	30.5	0.4 %	380	2.4 %	606	350	200	3.4 %	581	260	350	0.31	6.8	S	
	212	Joh et al. (1990)	NRC-J1	Exterior	51.5	0.6 %	815	3.2 %	1091	250	200	2.4 %	1091	250	250	0.02	11.4	S	
	213	Joh et al. (1990)	NRC-J2	Exterior	81.8	0.6 %	815	3.2 %	1091	250	200	2.4 %	1091	250	250	0.02	13.1	S	
53	214	Joh et al. (1990)	NRC-J4	Exterior	88.9	0.6 %	815	3.2 %	1091	250	200	2.4 %	1091	250	250	0.30	14.5	S	
	215	Joh et al. (1990)	NRC-J3	Exterior	86.9	0.3 %	840	3.2 %	1091	250	200	2.4 %	1091	250	250	0.02	13.3	S	
	216	Joh et al. (1991)	JXO-B1	Interior	21.3	0.2 %	307	0.8 %	371	350	150	1.1 %	371	300	300	0.16	4.3	Unknown	
	54	217	Joh et al. (1991b)	JX0-B8LH	Interior	26.9	0.2 %	377	0.6 %	404	350	200	2.0 %	404	300	300	0.15	3.7	Unknown
		218	Joh et al. (1991b)	JX0-B8MH	Interior	28.1	0.4 %	377	0.6 %	404	350	200	2.0 %	404	300	300	0.14	4.1	Unknown
	55	219	Joh et al. (1992)	NRC-J8	Exterior	53.7	0.2 %	717	2.5 %	675	250	200	2.8 %	675	250	250	0.02	7.1	S
		220	Joh et al. (1992)	NRC-J12	Exterior	83.7	0.2 %	717	2.5 %	698	250	200	2.4 %	698	250	250	0.02	12.8	S
221		Joh et al. (1992)	NRC-J14	Exterior	64.9	0.2 %	717	2.5 %	547	250	200	2.4 %	698	250	250	0.02	7.8	S-F	
222		Joh et al. (1992)	NRC-J10	Exterior	65.7	0.2 %	760	1.7 %	675	250	200	2.0 %	675	250	250	0.02	6.4	S-F	
223		Joh et al. (1992)	NRC-J11	Exterior	78.7	0.2 %	760	1.1 %	675	250	200	2.0 %	675	250	250	0.02	5.9	S-F	
224		Joh et al. (1992)	NRC-J5	Exterior	58.1	0.6 %	762	2.4 %	753	250	200	2.4 %	1092	250	250	0.02	10.9	S-F	
225		Joh et al. (1992)	NRC-J6	Exterior	32.2	0.6 %	762	2.4 %	753	250	200	2.4 %	1092	250	250	0.02	7.2	S-F	
56	226	Joh et al. (1992)	NRC-J7	Exterior	57.7	0.6 %	762	1.6 %	753	350	200	2.4 %	1092	250	250	0.02	10.0	S-F	
	227	Joh et al. (1992)	NRC-J9	Exterior	49.3	0.6 %	770	1.7 %	675	250	200	2.0 %	675	250	250	0.02	9.3	S	
	228	Joh et al. (1992)	NRC-J13	Exterior	79.4	0.6 %	770	2.5 %	698	250	200	2.4 %	698	250	250	0.02	11.1	S-F	
	229	Kaku and Asakusa (1991)	1	Exterior	31.1	0.5 %	250	1.6 %	381	220	160	1.6 %	360	220	220	0.17	6.2	S-F	
	230	Kaku and Asakusa (1991)	2	Exterior	41.7	0.5 %	250	1.6 %	381	220	160	1.6 %	360	220	220	0.10	6.2	S-F	
	231	Kaku and Asakusa (1991)	3	Exterior	41.7	0.5 %	250	1.6 %	381	220	160	1.6 %	360	220	220	0.00	5.3	S-F	
	232	Kaku and Asakusa (1991)	7	Exterior	32.2	0.5 %	250	1.6 %	381	220	160	1.8 %	395	220	220	0.12	6.3	S-F	
	233	Kaku and Asakusa (1991)	8	Exterior	41.2	0.5 %	250	1.6 %	381	220	160	1.8 %	395	220	220	0.08	6.1	S-F	
	234	Kaku and Asakusa (1991)	9	Exterior	40.6	0.5 %	250	1.6 %	381	220	160	1.8 %	395	220	220	0.00	6.0	S-F	
	235	Kaku and Asakusa (1991)	16	Exterior	37.4	0.5 %	250	1.6 %	381	220	160	3.2 %	381	220	220	0.00	6.1	S-F	
	236	Kaku and Asakusa (1991)	17	Exterior	39.7	0.5 %	250	1.6 %	381	220	160	1.1 %	395	220	220	0.00	4.4	S-F	
	237	Kaku and Asakusa (1991)	18	Exterior	40.7	0.5 %	250	1.6 %	381	220	160	0.8 %	282	220	220	0.00	3.0	S-F	
	238	Kaku and Asakusa (1991)	4	Exterior	44.7	0.1 %	281	1.6 %	381	220	160	1.6 %	360	220	220	0.17	6.0	S-F	
	239	Kaku and Asakusa (1991)	5	Exterior	36.7	0.1 %	281	1.6 %	381	220	160	1.6 %	360	220	220	0.09	5.2	S-F	
57	240	Kaku and Asakusa (1991)	6	Exterior	40.4	0.1 %	281	1.6 %	381	220	160	1.6 %	360	220	220	0.00	5.1	S-F	
	241	Kaku and Asakusa (1991)	10	Exterior	44.4	0.1 %	281	1.6 %	381	220	160	1.8 %	395	220	220	0.17	6.1	S-F	
	242	Kaku and Asakusa (1991)	11	Exterior	41.9	0.1 %	281	1.6 %	381	220	160	1.8 %	395	220	220	0.08	6.0	S-F	
	243	Kaku and Asakusa (1991)	12	Exterior	35.1	0.1 %	281	1.6 %	381	220	160	1.8 %	395	220	220	0.00	5.0	S-F	
	244	Kaku and Asakusa (1991)	14	Exterior	41.0	0.1 %	281	1.6 %	381	220	160	1.6 %	381	220	220	0.08	5.9	S-F	
	245	Kaku and Asakusa (1991)	15	Exterior	39.7	0.1 %	281	1.6 %	381	220	160	1.6 %	381	220	220	0.08	6.0	S-F	
	246	Kaku et al. (1993)	J11A	Interior	57.6	0.5 %	893	2.2 %	371	350	260	3.3 %	371	400	300	0.24	9.7	S-F	
	247	Kaku et al. (1993)	J12A	Interior	56.6	0.5 %	893	3.0 %	371	350	260	3.3 %	371	400	300	0.25	12.5	S-F	
	248	Kaku et al. (1993)	J31A	Interior	55.2	0.5 %	893	2.5 %	363	350	260	3.3 %	371	400	300	0.25	11.6	S-F	
	249	Kaku et al. (1993)	J32A	Interior	55.2	0.6 %	893	3.2 %	363	350	260	3.3 %	371	400	300	0.25	12.0	S-F	

(continued on next page)

Table A1 (continued)

No. of studies	S.N	Research Studies	Specimen	Joint Type	$f'_c$ (MPa)	$\rho_{jt}$	$f_{jit}$ (MPa)	$\rho_b$	$f_{yb}$ (MPa)	$h_b$ (mm)	$b_b$ (mm)	$\rho_c$	$f_{yc}$ (MPa)	$h_c$ (mm)	$b_c$ (mm)	ALF	$\tau_{exp}$	Failure Mode	
58	250	Kamimura et al. (2004)	NN.1	Interior	36.2	0.4 %	344	1.8 %	345	250	180	1.8 %	380	250	350	0.03	6.5	S-F	
59	251	Kanada et al. (1984)	U40L	Exterior	24.3	0.0 %	0	1.7 %	387	380	260	2.6 %	385.0	300	300	0.00	3.7	S	
	252	Kanada et al. (1984)	U20L	Exterior	26.7	0.0 %	0	0.9 %	387	380	260	1.3 %	387.0	300	300	0.00	3.4	B	
	253	Kanada et al. (1984)	U41L	Exterior	26.7	0.4 %	387	1.7 %	387	380	260	2.6 %	385	300	300	0.00	4.0	S-F	
	254	Kanada et al. (1984)	U42L	Exterior	30.1	0.8 %	387	1.7 %	387	380	260	2.6 %	385	300	300	0.00	4.0	S-F	
60	255	Karayannis and Sirkelis (2005)	AJ1s	Exterior	32.8	0.2 %	580	0.5 %	580	300	200	0.7 %	580	200	200	0.05	3.0	Unknown	
61	256	Karayannis et al. (1998)	Jo0	Exterior	20.8	0.0 %	0	0.5 %	580	200	100	1.6 %	580	200	100	0.10	3.7	S	
62	257	Karayannis et al. (2008)	A0	Exterior	31.6	0.0 %	0	0.5 %	580	300	200	0.5 %	580	200	200	0.05	2.6	S	
	258	Karayannis et al. (2008)	C0	Exterior	31.6	0.0 %	0	1.5 %	580	300	200	1.3 %	580	300	200	0.05	3.6	S	
	259	Karayannis et al. (2008)	B0	Exterior	31.6	0.0 %	0	1.6 %	580	300	200	0.5 %	580	300	200	0.05	4.2	S	
	260	Karayannis et al. (2008)	A1	Exterior	31.6	0.2 %	580	0.5 %	580	300	200	0.9 %	580	200	200	0.05	2.3	Unknown	
	261	Karayannis et al. (2008)	A2	Exterior	31.6	0.2 %	580	0.5 %	580	300	200	0.9 %	580	200	200	0.05	2.3	Unknown	
	262	Karayannis et al. (2008)	A3	Exterior	31.6	0.2 %	580	0.5 %	580	300	200	0.9 %	580	200	200	0.05	2.3	Unknown	
	263	Karayannis et al. (2008)	C2	Exterior	31.6	0.2 %	580	1.5 %	580	300	200	1.7 %	580	300	200	0.05	4.4	Unknown	
	264	Karayannis et al. (2008)	B1	Exterior	31.6	0.2 %	580	1.6 %	580	300	200	0.6 %	580	300	200	0.05	4.6	Unknown	
	265	Karayannis et al. (2008)	C2	Exterior	31.6	0.4 %	580	1.5 %	580	300	200	1.7 %	580	300	200	0.05	4.4	Unknown	
	266	Karayannis et al. (2008)	C2	Exterior	31.6	0.4 %	580	1.5 %	580	300	200	1.7 %	580	300	200	0.05	4.4	Unknown	
	63	267	Kashiwazaki et al. (1992)	MKJ-1	Interior	84.3	0.9 %	675	1.1 %	771	300	200	0.9 %	644	300	300	0.10	11.1	S-F
		268	Kashiwazaki et al. (1992)	MKJ-2	Interior	84.3	0.9 %	675	1.7 %	771	300	200	2.7 %	718	300	300	0.07	13.0	S-F
269		Kashiwazaki et al. (1992)	MKJ-3	Interior	98.5	0.9 %	675	1.5 %	742	300	200	1.7 %	794	300	300	0.07	13.0	S-F	
270		Kashiwazaki et al. (1992)	MKJ-4	Interior	98.5	0.9 %	675	2.2 %	742	300	200	3.8 %	771	300	300	0.07	14.6	S-F	
64	271	Kawai et al. (1997)	O8V	Exterior	88.1	0.3 %	928	2.4 %	522	450	325	2.7 %	522	475	475	0.67	10.6	S-F	
	272	Kawai et al. (1997)	I8C	Interior	85.5	0.3 %	928	2.7 %	522	450	325	2.7 %	522	475	475	0.20	12.4	S-F	
65	273	Khan et al. (2018)	TC	Exterior	30.0	0.0 %	0	5.0 %	605	250	200	3.8 %	605	250	200	0.03	5.6	Unknown	
66	274	Kitayama et al. (1991)	B3	Interior	24.5	0.9 %	235	1.7 %	311	300	200	2.3 %	371	300	300	0.08	6.9	S-F	
	275	Kitayama et al. (1991)	A1	Interior	30.6	0.6 %	320	2.1 %	780	300	200	3.5 %	539	300	300	0.06	9.2	S-F	
	276	Kitayama et al. (1991)	A4	Interior	30.6	0.6 %	320	1.5 %	780	300	200	3.5 %	539	300	300	0.06	9.9	S-F	
	277	Kitayama et al. (1991)	J1	Interior	25.7	0.3 %	368	2.0 %	401	300	200	2.3 %	401	300	300	0.08	7.3	S-F	
	67	278	Kitayama et al. (1992)	I5	Interior	85.4	0.4 %	250	1.5 %	769	300	200	3.5 %	534	300	300	0.02	10.7	S-F
279		Kitayama et al. (1992)	I6	Interior	85.4	0.4 %	250	1.7 %	772	300	200	3.5 %	534	300	300	0.02	13.5	S-F	
280		Kitayama et al. (1992)	I1	Interior	98.8	0.4 %	360	3.3 %	799	300	200	5.1 %	747	300	300	0.04	24.7	S-F	
281		Kitayama et al. (1992)	I3	Interior	41.4	0.4 %	360	2.4 %	799	300	200	3.5 %	361	300	300	0.03	11.9	S-F	
68		282	Kitayama et al. (2000)	PB-1	Interior	21.0	0.7 %	404	2.4 %	534	380	250	5.1 %	517	350	350	0.34	8.4	S-F
	283	Kitayama et al. (2000)	PNB-2	Interior	21.0	0.7 %	404	2.4 %	534	380	250	5.1 %	517	350	350	0.34	8.2	S-F	
	284	Kitayama et al. (2000)	PNB-3	Interior	21.9	0.7 %	404	2.4 %	534	380	250	5.1 %	517	350	350	0.33	7.8	S-F	
69	285	Kordina (1984)	RE4	Exterior	32.0	0.3 %	250	1.1 %	420	300	200	2.0 %	420	200	200	0.04	4.2	S	
70	286	Kotsovou (2011)	S5	Exterior	35.0	0.9 %	571	1.9 %	587	450	300	4.1 %	560	300	300	0.00	7.9	Unknown	
	287	Kotsovou (2011)	S2'	Exterior	35.0	1.2 %	571	1.9 %	587	450	300	3.9 %	560	300	300	0.00	8.0	Unknown	
71	288	Kotsovou (2012)	S10	Exterior	35.0	0.4 %	571	1.0 %	563	450	300	3.2 %	563	400	400	0.00	2.2	Unknown	
	289	Kotsovou (2012)	S6	Exterior	35.0	0.4 %	571	2.0 %	563	450	300	1.9 %	570	400	400	0.00	4.5	Unknown	
	290	Kotsovou (2012)	S9	Exterior	35.0	0.5 %	571	2.0 %	563	450	300	1.9 %	563	400	400	0.00	4.5	Unknown	
72	291	Kuang and Wong (2006)	BS-LL	Exterior	42.1	0.0 %	0	1.6 %	520	450	260	2.2 %	520	300	300	0.14	5.0	Unknown	
	292	Kuang and Wong (2006)	BS-L-LS	Exterior	31.6	0.0 %	0	1.6 %	520	450	260	2.2 %	520	300	300	0.14	4.3	Unknown	
	293	Kuang and Wong (2006)	BS-U	Exterior	31.0	0.0 %	0	1.6 %	520	450	260	2.2 %	520	300	300	0.14	4.3	Unknown	
73	294	Kulkarni and Li (2007)	JA	Interior	33.7	0.0 %	0	1.1 %	484	500	250	1.6 %	484	400	400	0.30	8.3	Unknown	
	295	Kulkarni and Li (2007)	JB	Interior	34.8	0.0 %	0	1.1 %	484	500	250	1.6 %	484	400	400	0.30	8.3	Unknown	
74	296	Kurose et al. (1991)	J1	Interior	24.1	0.7 %	550	1.1 %	463	508	406	2.4 %	463	508	508	0.00	8.6	Unknown	
75	297	Kurusu (1988)	NO4	Interior	34.1	0.1 %	354	1.2 %	388	300	200	2.3 %	388	300	300	0.06	6.2	Unknown	
76	298	Kusuhara et al. (2004)	JE-0	Interior	27.0	0.3 %	364	1.6 %	387	300	180	2.3 %	345	280	320	0.00	6.9	Unknown	
77	299	Lee and Ko (2007)	S0	Exterior	32.6	0.7 %	471	2.3 %	471	450	300	1.9 %	471	400	600	0.09	3.9	Unknown	
	300	Lee and Ko (2007)	S50	Exterior	34.2	0.7 %	471	2.3 %	471	450	300	1.9 %	471	400	600	0.09	3.8	Unknown	
	301	Lee and Ko (2007)	W0	Exterior	28.9	1.0 %	471	2.3 %	471	450	300	1.9 %	471	600	400	0.10	4.8	Unknown	
	302	Lee and Ko (2007)	W75	Exterior	30.4	1.0 %	471	2.3 %	471	450	300	1.9 %	471	600	400	0.10	4.9	Unknown	

(continued on next page)

Table A1 (continued)

No. of studies	S.N	Research Studies	Specimen	Joint Type	$f'_c$ (MPa)	$\rho_{jt}$	$f_{jit}$ (MPa)	$\rho_b$	$f_{yb}$ (MPa)	$h_b$ (mm)	$b_b$ (mm)	$\rho_c$	$f_{jc}$ (MPa)	$h_c$ (mm)	$b_c$ (mm)	ALF	$\tau_{exp}$	Failure Mode
	303	Lee and Ko (2007)	W150	Exterior	29.1	1.0 %	471	2.3 %	471	450	300	1.9 %	471	600	400	0.10	4.9	Unknown
78	304	Lee and Lee (2000)	EJ + 0.0	Exterior	19.0	0.3 %	673	1.5 %	451	300	200	2.7 %	451	300	300	0.00	3.5	S
79	305	Lee and Lee (2000)	EJ + 0.1	Exterior	19.0	0.3 %	673	1.5 %	451	300	200	2.7 %	451	300	300	0.10	3.7	S
80	306	Lee and Lee (2001)	HJ2-0.0	Exterior	38.0	0.2 %	671	2.2 %	540	300	200	2.7 %	504	300	300	0.00	6.3	S
	307	Lee and Lee (2001)	HJ2-0.15	Exterior	38.0	0.2 %	671	2.2 %	540	300	200	2.7 %	504	300	300	0.15	6.4	S
	308	Lee and Lee (2001)	HJ2-0.3	Exterior	38.0	0.2 %	671	2.2 %	540	300	200	2.7 %	504	300	300	0.30	5.9	S
	309	Lee and Lee (2001)	HJ5-0.0	Exterior	38.0	0.6 %	671	2.2 %	540	300	200	2.7 %	504	300	300	0.00	7.0	S
	310	Lee and Lee (2001)	HJ5-0.15	Exterior	38.0	0.6 %	671	2.2 %	540	300	200	2.7 %	504	300	300	0.15	6.1	S
	311	Lee and Lee (2001)	HJ5-0.3	Exterior	38.0	0.6 %	671	2.2 %	540	300	200	2.7 %	504	300	300	0.30	5.6	S
	312	Lee and Lee (2001)	NJ2-0.0	Exterior	23.5	0.2 %	671	1.6 %	442	300	200	2.7 %	504	300	300	0.00	4.6	S
	313	Lee and Lee (2001)	NJ2-0.15	Exterior	23.5	0.2 %	671	1.6 %	442	300	200	2.7 %	504	300	300	0.15	4.4	S
	314	Lee and Lee (2001)	NJ2-0.3	Exterior	23.5	0.2 %	671	1.6 %	442	300	200	2.7 %	504	300	300	0.30	4.4	S
	315	Lee and Lee (2001)	NJ5-0.0	Exterior	23.5	0.6 %	671	1.6 %	442	300	200	2.7 %	504	300	300	0.00	4.8	S
	316	Lee and Lee (2001)	NJ5-0.15	Exterior	23.5	0.6 %	671	1.6 %	442	300	200	2.7 %	504	300	300	0.15	4.5	S
	317	Lee and Lee (2001)	NJ5-0.3	Exterior	23.5	0.6 %	671	1.6 %	442	300	200	2.7 %	504	300	300	0.30	4.5	S
81	318	Lee et al. (2009)	J1	Interior	40.0	0.8 %	510	2.1 %	510	400	300	6.3 %	514	350	350	0.00	11.8	S
	319	Lee et al. (2009)	BJ1	Interior	40.0	0.8 %	510	1.2 %	510	400	300	6.3 %	514	350	350	0.00	10.4	S-F
82	320	Lee et al. (2010)	J10	Interior	27.0	0.0 %	0	0.9 %	456	600	300	2.5 %	456	400	400	0.19	6.2	S
	321	Lee et al. (2010)	A1	Interior	32.3	0.0 %	0	0.6 %	503	600	300	2.5 %	460	300	900	0.00	4.7	S
	322	Lee et al. (2010)	M1	Interior	32.0	0.1 %	499	0.6 %	503	600	300	2.5 %	460	300	900	0.00	4.7	S-F
83	323	Leon (1990)	BCJ2	Interior	27.6	0.5 %	414	0.9 %	414	305	203	2.8 %	414	254	254	0.00	2.8	S-F
	324	Leon (1990)	BCJ3	Interior	27.6	0.4 %	414	0.9 %	414	305	203	2.3 %	414	254	305	0.00	6.7	S-F
84	325	Le-Trung et al. (2010)	SD	Exterior	36.5	0.3 %	324	1.8 %	324	200	134	1.5 %	324	167	167	0.00	4.1	Unknown
	326	Le-Trung et al. (2010)	NS	Exterior	33.8	0.0 %	0	1.2 %	324	200	134	1.5 %	324	167	167	0.00	3.3	S
85	327	Liu (2006)	RC-1	Exterior	19.4	0.0 %	0	0.8 %	324	300	200	0.9 %	324	230	230	0.07	2.6	S-F
	328	Liu (2006)	RC-6	Exterior	25.9	0.1 %	384	0.6 %	307	330	250	1.8 %	307	250	250	0.06	2.8	S-F
	329	Liu (2006)	NZ-7	Exterior	30.0	1.7 %	384	0.6 %	307	330	250	1.8 %	307	250	250	0.00	3.5	Unknown
86	330	Liu and Park (1998)	Unit 2	Interior	48.9	0.0 %	0	1.0 %	321	500	300	2.0 %	321	300	460	0.12	5.6	S-F
87	331	Matsumoto et al. (2010)	B-0	Interior	54.6	0.5 %	1276	2.0 %	522	400	250	2.2 %	746	400	450	0.20	11.9	Unknown
	332	Matsumoto et al. (2010)	J-0	Interior	54.6	0.5 %	1276	2.0 %	710	400	250	2.2 %	746	400	450	0.20	13.6	Unknown
88	333	Megget (1971)	Unit 1	Exterior	28.3	0.6 %	317	1.3 %	286	460	255	1.2 %	305	380	330	0.00	3.9	S-F
89	334	Megget (1974)	Unit A	Exterior	22.1	1.6 %	317	1.7 %	374	460	255	2.5 %	365	380	330	0.07	5.4	S-F
90	335	Meinheit and Jirsa (1981)	1	Interior	26.2	0.5 %	409	2.2 %	449	457	279	2.1 %	457	457	330	0.40	7.8	S
	336	Meinheit and Jirsa (1981)	2	Interior	41.8	0.5 %	409	2.2 %	449	457	279	4.3 %	449	457	330	0.25	11.4	S
	337	Meinheit and Jirsa (1981)	3	Interior	26.6	0.5 %	409	2.2 %	449	457	279	6.7 %	402	457	330	0.39	8.7	S
	338	Meinheit and Jirsa (1981)	4	Interior	36.1	0.4 %	409	1.5 %	449	457	406	4.3 %	438	330	457	0.30	10.2	S
	339	Meinheit and Jirsa (1981)	5	Interior	35.9	0.5 %	409	2.2 %	449	457	279	4.3 %	449	457	330	0.04	10.9	S
	340	Meinheit and Jirsa (1981)	6	Interior	36.7	0.5 %	409	2.2 %	449	457	279	4.3 %	449	457	330	0.48	11.8	S-F
	341	Meinheit and Jirsa (1981)	7	Interior	37.2	0.4 %	409	1.5 %	449	457	406	4.3 %	438	330	457	0.47	10.3	S
	342	Meinheit and Jirsa (1981)	13	Interior	41.3	1.5 %	409	2.2 %	449	457	279	4.3 %	449	457	330	0.25	11.1	S
	343	Meinheit and Jirsa (1981)	14	Interior	33.2	1.1 %	409	1.5 %	449	457	406	4.3 %	438	330	457	0.32	10.6	S
	344	Meinheit and Jirsa (1981)	12	Interior	35.2	2.4 %	423	2.2 %	449	457	279	4.3 %	449	457	330	0.30	14.0	S-F
91	345	Melo et al. (2012)	TPA-1	Exterior	24.4	0.0 %	0	0.7 %	405	400	250	0.7 %	405	250	250	0.13	3.6	S
	346	Melo et al. (2012)	TPA-2	Exterior	25.8	0.0 %	0	0.7 %	405	400	250	0.7 %	405	250	250	0.12	3.6	S
	347	Melo et al. (2012)	TP-B1	Exterior	15.8	0.0 %	0	0.7 %	405	400	250	0.7 %	405	250	250	0.20	3.6	S
	348	Melo et al. (2012)	TPB-2	Exterior	27.3	0.0 %	0	0.7 %	405	400	250	0.7 %	405	250	250	0.12	3.6	S
	349	Melo et al. (2012)	TPC	Exterior	23.8	0.0 %	0	0.7 %	405	400	250	0.7 %	405	250	250	0.14	3.6	S
	350	Melo et al. (2012)	TD	Exterior	20.8	0.0 %	0	0.7 %	465	400	250	0.7 %	465	250	250	0.15	3.7	S
92	351	Morita et al. (2004)	M1	Interior	17.1	0.3 %	344	1.9 %	520	400	300	5.9 %	520	350	300	0.00	6.3	S
	352	Morita et al. (2004)	M2	Interior	18.2	0.3 %	344	1.9 %	520	400	300	5.9 %	520	350	300	0.00	6.9	S
	353	Morita et al. (2004)	M3	Interior	18.8	0.3 %	344	1.9 %	520	400	300	5.9 %	520	350	300	0.00	6.3	S
	354	Morita et al. (2004)	M6	Interior	19.4	0.3 %	344	1.3 %	520	400	300	5.9 %	520	350	300	0.00	6.6	S
	355	Morita et al. (2004)	M4	Interior	20.6	2.1 %	429	1.9 %	520	400	300	5.9 %	520	350	300	0.00	7.6	S
93	356	Murty et al. (2003)	Q1	Exterior	25.6	0.0 %	0	1.6 %	382	400	200	2.4 %	382	250	200	0.00	6.3	S

(continued on next page)



Table A1 (continued)

No. of studies	S.N	Research Studies	Specimen	Joint Type	$f'_c$ (MPa)	$\rho_{jt}$	$f_{jit}$ (MPa)	$\rho_b$	$f_{yb}$ (MPa)	$h_b$ (mm)	$b_b$ (mm)	$\rho_c$	$f_{jc}$ (MPa)	$h_c$ (mm)	$b_c$ (mm)	ALF	$\tau_{exp}$	Failure Mode
	357	Murty et al. (2003)	P1	Exterior	27.3	0.0 %	0	1.6 %	382	400	200	2.4 %	382	250	200	0.00	6.9	S
	358	Murty et al. (2003)	R1	Exterior	30.2	0.0 %	0	1.6 %	382	400	200	2.4 %	382	250	200	0.00	7.0	S
	359	Murty et al. (2003)	S1	Exterior	27.8	0.0 %	0	1.6 %	382	400	200	2.4 %	382	250	200	0.00	6.6	S
	360	Murty et al. (2003)	P2	Exterior	26.3	2.3 %	382	1.6 %	382	400	200	2.4 %	382	250	200	0.00	8.2	S
	361	Murty et al. (2003)	P3	Exterior	27.0	2.3 %	382	1.6 %	382	400	200	2.4 %	382	250	200	0.00	7.3	S
	362	Murty et al. (2003)	Q2	Exterior	27.2	2.3 %	382	1.6 %	382	400	200	2.4 %	382	250	200	0.00	8.9	S
	363	Murty et al. (2003)	Q3	Exterior	26.9	2.3 %	382	1.6 %	382	400	200	2.4 %	382	250	200	0.00	8.6	S
	364	Murty et al. (2003)	R2	Exterior	27.3	2.3 %	382	1.6 %	382	400	200	2.4 %	382	250	200	0.00	9.3	S
	365	Murty et al. (2003)	R3	Exterior	27.1	2.3 %	382	1.6 %	382	400	200	2.4 %	382	250	200	0.00	8.8	S
	366	Murty et al. (2003)	S2	Exterior	26.8	2.3 %	382	1.6 %	382	400	200	2.4 %	382	250	200	0.00	8.8	S
	367	Murty et al. (2003)	S3	Exterior	30.1	2.3 %	382	1.6 %	382	400	200	2.4 %	382	200	250	0.00	8.0	S
94	368	Nakamura et al. (1991)	No.5	Interior	64.1	1.2 %	873	1.7 %	785	400	300	2.2 %	785	400	400	0.10	16.3	S-F
	369	Nakamura et al. (1991)	No.6	Interior	63.1	1.2 %	873	1.7 %	785	400	300	2.2 %	785	400	400	0.10	17.3	S-F
	370	Nakamura et al. (1991)	No.7	Interior	76.0	1.2 %	873	1.7 %	785	400	300	2.2 %	785	400	400	0.08	16.8	S-F
	371	Nakamura et al. (1991)	No.1	Interior	65.3	0.4 %	880	1.7 %	582	400	300	2.2 %	785	400	400	0.09	12.6	S-F
	372	Nakamura et al. (1991)	No.2	Interior	68.4	0.4 %	880	1.7 %	785	400	300	2.2 %	785	400	400	0.09	15.3	S
	373	Nakamura et al. (1991)	No.4	Interior	91.9	0.4 %	880	1.7 %	785	400	300	2.2 %	785	400	400	0.07	17.1	S-F
95	374	Nishi et al. (1992)	JO-2	Interior	24.9	0.4 %	448	1.6 %	366	150	120	2.3 %	366	150	150	0.70	6.3	Unknown
96	375	Nishiyama et al. (1989)	RC2	Exterior	29.8	0.8 %	335	2.5 %	425	300	200	3.2 %	425	300	300	0.04	6.3	S-F
97	376	Noguchi and Kuruusu (1988)	NO2	Interior	34.1	0.1 %	354	1.5 %	325	300	200	2.3 %	388	300	300	0.06	5.5	Unknown
98	377	Noguchi and Kashiwazaki (1992)	OKJ-1	Interior	70.0	0.9 %	955	2.3 %	718	300	200	2.8 %	718	300	300	0.12	14.4	S-F
	378	Noguchi and Kashiwazaki (1992)	OKJ-4	Interior	70.0	0.9 %	955	1.8 %	718	300	200	2.8 %	718	300	300	0.12	15.1	S-F
	379	Noguchi and Kashiwazaki (1992)	OKJ-5	Interior	70.0	0.9 %	955	2.5 %	718	300	200	3.4 %	718	300	300	0.12	14.8	S
	380	Noguchi and Kashiwazaki (1992)	OKJ-6	Interior	53.5	0.9 %	955	2.0 %	718	300	200	2.8 %	718	300	300	0.12	13.2	S
99	381	Ogawa et al. (2003)	BUCS	Exterior	18.6	0.4 %	402	1.0 %	388	400	260	2.7 %	388	300	300	0.20	4.0	S
	382	Ogawa et al. (2003)	BUVS	Exterior	18.6	0.4 %	402	1.0 %	389	400	260	2.7 %	388	300	300	0.62	3.4	S
100	383	Oh et al. (1992)	EJS-200-0	Exterior	26.8	0.0 %	0	2.5 %	434	200	140	2.7 %	417	200	200	0.00	4.9	S
	384	Oh et al. (1992)	EJS-400-0	Exterior	41.7	0.0 %	0	2.5 %	434	200	140	2.7 %	417	200	200	0.00	6.3	S
	385	Oh et al. (1992)	EJS-200-0.3 N	Exterior	26.8	0.4 %	375	2.5 %	434	200	140	2.7 %	417	200	200	0.00	5.5	Unknown
	386	Oh et al. (1992)	EJS-200-2-0.6 N'	Exterior	24.0	0.7 %	375	2.5 %	434	200	140	2.7 %	417	200	200	0.00	5.7	Unknown
	387	Oh et al. (1992)	EJS-200-2-0.6 N	Exterior	24.0	0.4 %	375	2.5 %	434	200	140	3.1 %	417	200	200	0.00	5.6	Unknown
	388	Oh et al. (1992)	EJS-400-0.3 N	Exterior	41.7	0.4 %	375	2.5 %	434	200	140	2.7 %	417	200	200	0.00	6.8	Unknown
	389	Oh et al. (1992)	EJS-400-0.6 N'	Exterior	44.6	0.7 %	375	2.5 %	434	200	140	2.7 %	417	200	200	0.00	7.0	Unknown
	390	Oh et al. (1992)	EJS-400-0.6 N	Exterior	44.6	0.4 %	375	2.5 %	434	200	140	3.1 %	417	200	200	0.00	7.0	Unknown
	391	Oh et al. (1992)	EJS-400-0.6H	Exterior	43.1	0.9 %	765	3.6 %	417	200	140	2.7 %	417	200	200	0.00	8.4	Unknown
	392	Oh et al. (1992)	EJS-400-1.2H	Exterior	43.1	1.8 %	765	3.6 %	417	200	140	2.7 %	417	200	200	0.00	9.1	Unknown
101	393	Ohwada (1970)	No. 1	Interior	21.5	0.0 %	0	1.3 %	392	300	150	3.2 %	392	200	200	0.18	6.1	Unknown
102	394	Ohwada (1970)	No. 3	Interior	21.5	0.7 %	245	1.3 %	392	300	150	3.2 %	392	200	200	0.18	6.9	S
	395	Ohwada (1970)	No. 2	Interior	21.5	0.3 %	245	1.3 %	392	300	150	3.2 %	392	200	200	0.18	7.6	S
103	396	Ohwada (1973)	P-1	Interior	11.6	0.0 %	0	1.5 %	400	300	150	4.0 %	400	200	200	0.34	3.7	S
	397	Ohwada (1973)	P-2	Interior	13.3	0.0 %	0	1.3 %	385	300	150	3.2 %	385	200	200	0.29	4.2	S
	398	Ohwada (1973)	P-3	Interior	12.8	0.0 %	0	1.0 %	385	300	150	3.2 %	385	200	200	0.31	4.3	S
	399	Ohwada (1973)	P-4	Interior	13.4	0.7 %	245	1.3 %	385	300	150	3.2 %	385	200	200	0.29	4.3	S-F
104	400	Ohwada (1976)	JO-0	Interior	20.1	0.0 %	0	3.9 %	402	150	100	3.4 %	402	150	100	0.00	7.6	S
105	401	Ohwada (1977)	JO-1	Interior	20.0	0.0 %	0	2.0 %	432	150	150	3.4 %	432	150	150	0.00	6.1	S
	402	Ohwada (1977)	JO-2	Interior	20.0	0.4 %	450	2.0 %	432	150	150	3.4 %	432	150	150	0.00	7.3	S
106	403	Ohwada (1980)	JO-3	Interior	20.6	0.0 %	0	2.0 %	394	150	150	3.4 %	394	150	150	0.00	6.9	S

(continued on next page)

Table A1 (continued)

No. of studies	S.N	Research Studies	Specimen	Joint Type	$f'_c$ (MPa)	$\rho_{jt}$	$f_{jit}$ (MPa)	$\rho_b$	$f_{yb}$ (MPa)	$h_b$ (mm)	$b_b$ (mm)	$\rho_c$	$f_{yc}$ (MPa)	$h_c$ (mm)	$b_c$ (mm)	ALF	$\tau_{exp}$	Failure Mode
	404	Ohwada (1980)	JO-4	Interior	14.0	0.0 %	0	2.0 %	360	150	150	6.8 %	360	150	150	0.00	6.2	S
	405	Ohwada (1980)	LJO-1	Interior	20.0	0.0 %	0	2.0 %	372	150	150	6.8 %	372	150	150	0.00	6.6	S
	406	Ohwada (1980)	LJO-3	Interior	20.0	0.0 %	0	2.0 %	372	150	150	4.5 %	372	150	150	0.00	6.1	S
	407	Ohwada (1980)	LJO-2	Interior	20.0	0.3 %	407	2.0 %	372	150	150	6.8 %	372	150	150	0.00	6.5	S
107	408	Ohwada (1981)	LJO-4	Interior	17.1	0.0 %	0	1.8 %	368	200	120	2.3 %	368	150	150	0.16	5.0	S
	409	Ohwada (1981)	LJO-5	Interior	17.1	0.0 %	0	1.8 %	368	200	120	2.3 %	368	150	150	0.41	5.3	S-F
108	410	Oka and Shiohara (1992)	J-11	Interior	39.2	0.4 %	401	4.2 %	365	300	240	7.7 %	365	300	300	0.12	12.6	S
	411	Oka and Shiohara (1992)	J-10	Interior	39.2	0.4 %	598	1.9 %	687	300	240	3.4 %	687	300	300	0.12	10.8	S
	412	Oka and Shiohara (1992)	J-6	Interior	79.2	0.2 %	775	1.9 %	663	300	240	3.4 %	663	300	300	0.12	15.0	S-F
	413	Oka and Shiohara (1992)	J-8	Interior	79.2	0.4 %	775	4.3 %	364	300	240	7.7 %	364	300	300	0.12	17.0	S
	414	Oka and Shiohara (1992)	J-1	Interior	81.2	0.4 %	1374	1.9 %	627	300	240	3.4 %	627	300	300	0.11	14.1	S-F
	415	Oka and Shiohara (1992)	J-2	Interior	81.2	0.4 %	1374	1.7 %	1429	300	240	3.4 %	627	300	300	0.11	15.3	S
	416	Oka and Shiohara (1992)	J-4	Interior	72.8	0.4 %	1374	2.2 %	506	300	240	5.3 %	492	300	300	0.13	14.6	S-F
	417	Oka and Shiohara (1992)	J-5	Interior	72.8	0.4 %	1374	1.9 %	824	300	240	3.4 %	824	300	300	0.13	16.2	S
109	418	Onish et al. (1990)	No.1	Exterior	25.9	0.0 %	0	0.7 %	389	250	250	1.2 %	389	250	250	0.00	3.8	S-F
	419	Onish et al. (1990)	No.4	Exterior	25.2	0.0 %	0	1.2 %	389	250	250	1.2 %	389	250	250	0.00	3.7	S-F
	420	Onish et al. (1990)	No.2	Exterior	28.1	0.2 %	314	0.7 %	389	250	250	1.2 %	389	250	250	0.00	4.1	S-F
	421	Onish et al. (1990)	NO.5	Exterior	28.1	0.5 %	314	1.2 %	389	250	250	1.2 %	389	250	250	0.00	4.7	S-F
110	422	Oskouei (2010)	Specimen-1	Exterior	24.3	0.5 %	282	1.5 %	417	400	350	2.5 %	417	350	350	0.00	4.0	S
	423	Oskouei (2010)	Specimen-2	Exterior	19.6	0.5 %	282	1.5 %	417	400	350	2.5 %	417	350	350	0.00	4.3	S
111	424	Ota et al. (2004)	RC	Interior	74.2	0.2 %	944	2.2 %	538	400	280	2.5 %	538	400	400	0.08	12.5	S-F
112	425	Otani et al. (1984)	J1	Interior	25.7	0.3 %	368	2.0 %	401	300	200	2.3 %	401	300	300	0.08	7.3	S-F
	426	Otani et al. (1984)	J2	Interior	24.0	0.6 %	368	2.0 %	401	300	200	2.3 %	401	300	300	0.08	7.5	S-F
	427	Otani et al. (1984)	J3	Interior	24.0	1.7 %	368	2.0 %	401	300	200	2.3 %	401	300	300	0.08	8.0	S-F
	428	Otani et al. (1984)	J4	Interior	25.7	0.3 %	368	2.0 %	401	300	200	2.3 %	401	300	300	0.30	7.1	S-F
	429	Otani et al. (1984)	J5	Interior	28.7	0.3 %	368	2.0 %	401	300	200	2.3 %	401	300	300	0.07	7.2	S-F
113	430	Owada (1984)	LJO-6	Interior	28.9	0.0 %	0	1.8 %	357	200	120	2.3 %	357	150	150	0.23	8.1	Unknown
114	431	Owada (1992)	J0C-1	Interior	31.2	0.4 %	447	1.4 %	340	150	120	2.3 %	343	150	150	0.13	5.3	S-F
	432	Owada (1992)	J0R-1	Interior	31.2	0.4 %	447	1.4 %	340	150	120	2.3 %	343	150	150	0.13	8.3	S-F
115	433	Owada (2000)	JO-5	Interior	37.6	0.0 %	0	1.8 %	349	200	120	2.3 %	349	150	150	0.17	9.1	S
116	434	Ozaki et al. (2010)	1	Interior	32.8	0.4 %	338	2.2 %	410	300	180	1.8 %	410	300	300	0.09	8.6	S-F
117	435	Pantelides et al. (2002)	Unit 1	Exterior	33.1	0.0 %	0	3.1 %	459	406	406	2.5 %	470	406	406	0.10	5.2	B
	436	Pantelides et al. (2002)	Unit 2	Exterior	33.1	0.0 %	0	3.1 %	459	406	406	2.5 %	470	406	406	0.25	4.9	B
	437	Pantelides et al. (2002)	Unit 3	Exterior	34.0	0.0 %	0	3.1 %	459	406	406	2.5 %	470	406	406	0.10	5.0	S
	438	Pantelides et al. (2002)	Unit 4	Exterior	34.0	0.0 %	0	3.1 %	459	406	406	2.5 %	470	406	406	0.25	5.7	S
	439	Pantelides et al. (2002)	Unit 5	Exterior	31.7	0.0 %	0	3.1 %	459	406	406	2.5 %	470	406	406	0.10	5.2	S
	440	Pantelides et al. (2002)	Unit 6	Exterior	31.7	0.0 %	0	3.1 %	459	406	406	2.5 %	470	406	406	0.25	5.3	S
118	441	Park and Bullman (1997)	4b	Exterior	39.2	0.0 %	0	0.9 %	570	500	250	0.9 %	550	300	300	0.09	4.0	S
	442	Park and Bullman (1997)	4c	Exterior	36.8	0.0 %	0	0.9 %	570	500	250	0.9 %	550	300	300	0.17	4.0	S
	443	Park and Bullman (1997)	4d	Exterior	39.2	0.0 %	0	0.9 %	570	500	250	3.6 %	580	300	300	0.00	2.9	S
	444	Park and Bullman (1997)	4e	Exterior	40.0	0.0 %	0	0.9 %	570	500	250	3.6 %	580	300	300	0.10	3.8	S
	445	Park and Bullman (1997)	4f	Exterior	37.6	0.0 %	0	0.9 %	570	500	250	3.6 %	580	300	300	0.18	4.3	S
	446	Park and Bullman (1997)	5b	Exterior	43.2	0.5 %	480	0.9 %	485	500	250	2.2 %	485	300	300	0.08	5.5	S
119	447	Pessiki et al. (1990)	I-01	Interior	32.7	0.0 %	0	1.3 %	483	610	356	2.0 %	456	406	406	0.25	6.3	S-F
	448	Pessiki et al. (1990)	I-02	Interior	32.5	0.0 %	0	1.3 %	483	610	356	2.0 %	456	406	406	0.24	6.2	S-F
	449	Pessiki et al. (1990)	I-03	Interior	30.4	0.0 %	0	1.3 %	483	610	356	1.8 %	486	406	406	0.31	6.0	S-F
	450	Pessiki et al. (1990)	I-04	Interior	31.9	0.0 %	0	1.3 %	483	610	356	1.9 %	518	406	406	0.30	5.9	S-F
	451	Pessiki et al. (1990)	I-07	Interior	26.0	0.0 %	0	0.8 %	481	610	356	2.0 %	461	406	406	0.43	4.7	S-F
	452	Pessiki et al. (1990)	I-08	Interior	25.4	0.0 %	0	0.8 %	481	610	356	2.0 %	461	406	406	0.43	4.6	S-F
	453	Pessiki et al. (1990)	I-09	Interior	29.1	0.0 %	0	0.8 %	425	610	356	2.0 %	461	406	406	0.10	4.6	S-F
	454	Pessiki et al. (1990)	I-05	Interior	29.8	0.2 %	427	1.3 %	531	610	356	1.9 %	427	406	406	0.33	6.1	S-F
120	455	Pimanmas and Chaimahawan (2010)	J0	Interior	27.3	0.0 %	0	1.5 %	480	300	175	2.9 %	480	350	200	0.17	5.9	Unknown

(continued on next page)

Table A1 (continued)

No. of studies	S.N	Research Studies	Specimen	Joint Type	$f'_c$ (MPa)	$\rho_{jt}$	$f_{jit}$ (MPa)	$\rho_b$	$f_{yb}$ (MPa)	$h_b$ (mm)	$b_b$ (mm)	$\rho_c$	$f_{yc}$ (MPa)	$h_c$ (mm)	$b_c$ (mm)	ALF	$\tau_{exp}$	Failure Mode
121	456	Rajagopal and Prabavathy (2013)	A2-II	Exterior	23.0	0.7 %	410	1.3 %	410	300	200	0.8 %	410	200	300	0.00	4.6	Unknown
122	457	Realfonzo (2018)	Type 1	Exterior	16.0	0.0 %	0	1.6 %	540	400	300	0.7 %	540	300	300	0.21	3.5	Unknown
	458	Realfonzo (2018)	Type 2	Exterior	16.0	0.0 %	0	2.1 %	540	400	300	2.8 %	540	300	300	0.21	3.6	Unknown
123	459	Reys de Ortiz (1993)	BC1	Exterior	33.8	0.0 %	0	1.1 %	720	400	200	1.5 %	461	300	200	0.00	5.4	S
	460	Reys de Ortiz (1993)	BC3	Exterior	33.0	0.0 %	0	1.1 %	720	400	200	2.1 %	461	300	200	0.00	5.7	S
	461	Reys de Ortiz (1993)	BC5	Exterior	37.9	0.0 %	0	1.1 %	720	400	200	2.4 %	461	300	200	0.13	5.5	S
	462	Reys de Ortiz (1993)	BC6	Exterior	35.0	0.0 %	0	1.1 %	720	400	200	2.4 %	461	300	200	0.14	5.5	S
	463	Reys de Ortiz (1993)	BC2	Exterior	37.8	0.3 %	461	1.1 %	720	400	200	1.5 %	461	300	200	0.00	6.0	S
124	464	Sagbas (2007)	ED1	Exterior	31.1	0.0 %	0	1.4 %	349	508	305	2.8 %	335	381	381	0.09	4.5	S-F
125	465	Sanada and Li (2014)	J2	Exterior	20.2	0.0 %	0	1.4 %	373	450	300	2.5 %	373	300	300	0.00	3.9	Unknown
126	466	Sarsam and Phipps (1985)	EX2	Exterior	52.5	0.0 %	0	1.0 %	504	305	155	2.5 %	504	205	155	0.18	4.6	S
127	469	Scott (2007)	C7	Exterior	35.2	0.3 %	250	1.4 %	540	300	110	3.6 %	540	150	150	0.35	5.0	S
	470	Scott (2007)	C9	Exterior	35.9	0.3 %	250	1.4 %	540	300	110	3.6 %	540	150	150	0.34	4.4	S
	471	Scott (2007)	C1AL	Exterior	33.4	0.4 %	250	1.1 %	540	210	110	3.6 %	540	150	150	0.07	5.2	S
	472	Scott (2007)	C2	Exterior	49.4	0.4 %	250	1.1 %	540	210	110	3.6 %	540	150	150	0.25	5.1	S
	473	Scott (2007)	C3L	Exterior	35.5	0.4 %	250	1.1 %	540	210	110	3.6 %	540	150	150	0.06	5.1	S
	474	Scott (2007)	C4	Exterior	41.4	0.4 %	250	2.1 %	540	210	110	3.6 %	540	150	150	0.29	7.8	S
	475	Scott (2007)	C4A	Exterior	44.3	0.4 %	250	2.1 %	540	210	110	3.6 %	540	150	150	0.28	8.4	S
	476	Scott (2007)	C4AL	Exterior	35.8	0.4 %	250	2.1 %	540	210	110	3.6 %	540	150	150	0.06	7.5	S
	477	Scott (2007)	C6	Exterior	39.8	0.4 %	250	2.1 %	540	210	110	3.6 %	540	150	150	0.31	5.7	S
	478	Scott (2007)	C6L	Exterior	45.8	0.4 %	250	2.1 %	540	210	110	3.6 %	540	150	150	0.05	6.9	S
128	479	Shin et al. (1992)	HJC0-R0	Exterior	78.5	0.0 %	0	2.4 %	392	200	120	2.5 %	392	150	150	0.01	10.3	S-F
	480	Shin et al. (1992)	HJC1-R0	Exterior	78.5	0.4 %	235	2.4 %	392	200	120	2.5 %	392	150	150	0.01	11.1	S-F
129	481	Shinjo et al. (2009)	B-1	Interior	111.0	0.4 %	1452	2.8 %	549	400	300	2.2 %	528	400	400	0.10	20.2	S-F
	482	Shinjo et al. (2009)	J-1	Interior	110.0	0.4 %	1452	3.2 %	716	400	300	2.2 %	528	400	400	0.10	24.7	S
	483	Shinjo et al. (2009)	BJ-1	Interior	110.0	0.4 %	1452	3.2 %	549	400	300	2.2 %	528	400	400	0.10	22.4	S
	484	Shrestha et al. (2009)	UC-1	Exterior	25.8	0.0 %	0	2.7 %	532	450	300	2.0 %	532	300	300	0.08	2.4	0
130	485	Smith (1972)	Unit 5	Exterior	20.1	0.5 %	310	1.3 %	301	460	255	1.2 %	274	380	330	0.00	3.0	S-F
	486	Smith (1972)	Unit 6	Exterior	17.7	1.0 %	310	1.3 %	299	460	255	1.2 %	297	380	330	0.00	3.1	S-F
	487	Smith (1972)	Unit 4	Exterior	20.5	1.1 %	310	1.3 %	296	460	255	1.2 %	274	380	330	0.00	2.9	S-F
131	488	Supaviriyakit and Pimanmas (2008)	J1	Interior	26.3	0.0 %	0	1.6 %	480	300	175	2.9 %	480	350	200	0.13	6.2	S
132	489	Suzuki et al. (2002)	E00	Interior	24.0	0.4 %	358	1.8 %	384	500	230	1.4 %	384	500	400	0.25	6.6	S
133	490	Takeuchi et al. (2003)	O-5	Exterior	42.0	0.4 %	327	1.1 %	445	450	350	2.9 %	553	400	400	0.10	3.7	S
134	491	Taylor (1974)	C3/41/13Y	Exterior	22.4	0.4 %	250	1.3 %	500	200	100	4.1 %	500	140	140	0.55	4.9	S
	492	Taylor (1974)	P1/41/24	Exterior	26.4	0.4 %	250	2.4 %	500	200	100	4.1 %	500	140	140	0.46	6.6	S
	493	Taylor (1974)	P2/41/24	Exterior	29.0	0.4 %	250	2.4 %	500	200	100	4.1 %	500	140	140	0.42	8.0	S
	494	Taylor (1974)	P2/41/24A	Exterior	37.6	0.4 %	250	2.4 %	500	200	100	4.1 %	500	140	140	0.33	9.0	S
	495	Taylor (1974)	A3/41/24	Exterior	21.6	0.4 %	250	2.4 %	500	200	100	4.1 %	500	140	140	0.57	7.2	S
	496	Taylor (1974)	B3/41/24	Exterior	17.6	0.4 %	250	2.4 %	500	200	100	4.1 %	500	140	140	0.70	6.4	S
	497	Taylor (1974)	C3/41/24X	Exterior	40.0	0.4 %	250	2.4 %	500	200	100	4.1 %	500	140	140	0.31	6.2	S
	498	Taylor (1974)	C3/41/24Y	Exterior	48.0	0.4 %	250	2.4 %	500	200	100	4.1 %	500	140	140	0.26	8.3	S
	499	Taylor (1974)	D3/41/24	Exterior	42.2	0.4 %	250	2.4 %	500	200	100	4.1 %	500	140	140	0.07	9.6	S
	500	Taylor (1974)	C3/41/24BY	Exterior	25.6	0.7 %	250	2.4 %	500	200	100	4.1 %	500	140	140	0.48	5.5	S
135	501	Teroaka (1997)	NO4	Exterior	39.1	0.5 %	328	1.4 %	434	560	365	2.5 %	421	540	540	0.01	4.9	S-F
	502	Teroaka (1997)	NO10	Exterior	34.8	0.6 %	328	1.1 %	421	560	365	2.5 %	421	540	540	0.01	4.1	S-F
	503	Teroaka (1997)	NO3	Exterior	38.9	0.6 %	328	1.4 %	434	560	365	2.5 %	421	540	540	0.01	4.7	S-F
	504	Teroaka (1997)	NO26	Interior	35.6	0.6 %	300	1.9 %	399	300	260	2.1 %	399	340	340	0.17	9.4	S-F
	505	Teroaka (1997)	NO28	Interior	36.2	0.6 %	300	2.6 %	399	300	260	2.1 %	399	340	340	0.16	11.5	S
	506	Teroaka (1997)	NO29	Interior	44.0	0.6 %	300	1.9 %	399	300	260	2.1 %	399	340	340	0.23	9.5	S-F
136	507	Tsonos (1993)	S1	Exterior	37.0	0.8 %	495	1.1 %	485	300	200	2.3 %	485	200	200	0.40	6.9	S-F
	508	Tsonos (1993)	S2	Exterior	26.0	0.8 %	495	1.1 %	507	300	200	0.8 %	497	200	200	0.40	8.6	S-F
	509	Tsonos (1993)	S3	Exterior	19.0	0.8 %	495	1.3 %	497	300	200	0.8 %	507	200	200	0.40	9.5	S-F

(continued on next page)

Table A1 (continued)

No. of studies	S.N	Research Studies	Specimen	Joint Type	$f'_c$ (MPa)	$\rho_{jt}$	$f_{jit}$ (MPa)	$\rho_b$	$f_{yb}$ (MPa)	$h_b$ (mm)	$b_b$ (mm)	$\rho_c$	$f_{yc}$ (MPa)	$h_c$ (mm)	$b_c$ (mm)	ALF	$\tau_{exp}$	Failure Mode
	510	Tsonos (1993)	S4	Exterior	21.0	0.8 %	495	1.8 %	497	300	200	1.2 %	485	200	200	0.40	10.2	S
	511	Tsonos (1993)	S5	Exterior	25.0	0.8 %	495	2.1 %	507	300	200	1.9 %	466	200	200	0.40	10.9	S
	512	Tsonos (1993)	S6	Exterior	33.0	0.8 %	495	2.1 %	485	300	200	1.5 %	466	200	200	0.40	9.8	S
	513	Tsonos (1993)	P1	Exterior	16.0	0.8 %	495	2.1 %	485	300	200	3.1 %	466	200	200	0.40	9.5	S
	514	Tsonos (1993)	Y1	Exterior	23.0	0.8 %	495	2.1 %	485	300	200	1.5 %	478	200	200	0.40	8.9	S
	515	Tsonos (1993)	F1	Exterior	17.0	0.8 %	495	2.1 %	485	300	200	1.5 %	485	200	200	0.40	13.1	S
	516	Tsonos (1993)	O1	Exterior	20.0	0.8 %	495	2.1 %	485	300	200	1.5 %	485	200	200	0.40	9.8	S
	517	Tsonos (1993)	F2	Exterior	24.0	0.8 %	495	2.1 %	485	300	200	1.5 %	485	200	200	0.40	9.6	S
	518	Tsonos (1996)	MS4	Exterior	33.6	1.2 %	495	1.2 %	466	300	200	3.1 %	485	200	200	0.29	5.3	S-F
137	519	Tsonos (2002)	O1	Exterior	16.0	0.0 %	0	2.1 %	485	300	200	1.5 %	485	200	200	0.40	5.4	S
138	520	Tsonos (2007)	S1	Exterior	37.0	0.7 %	495	1.2 %	485	300	200	2.3 %	485	200	200	0.18	3.6	S-F
	521	Tsonos (2007)	S2	Exterior	26.0	0.7 %	495	1.2 %	465	300	200	0.8 %	465	200	200	0.18	3.7	S-F
	522	Tsonos (2007)	S3	Exterior	19.0	0.7 %	495	1.2 %	465	300	200	0.8 %	465	200	200	0.18	3.6	S-F
	523	Tsonos (2007)	S4	Exterior	21.0	0.7 %	495	2.0 %	485	300	200	1.2 %	465	200	200	0.18	3.9	S
	524	Tsonos (2007)	S5	Exterior	25.0	0.7 %	495	2.2 %	485	300	200	1.9 %	465	200	200	0.18	4.5	S
	525	Tsonos (2007)	S6	Exterior	33.0	0.7 %	495	2.2 %	485	300	200	1.5 %	485	200	200	0.18	4.6	S
	526	Tsonos (2007)	S6'	Exterior	29.0	0.7 %	495	2.2 %	485	300	200	3.1 %	485	200	200	0.18	5.3	S-F
	527	Tsonos (2007)	O1	Exterior	20.0	1.1 %	495	2.2 %	485	300	200	3.1 %	485	200	200	0.18	3.6	S
	528	Tsonos (2007)	F2	Exterior	24.0	1.1 %	495	2.2 %	485	300	200	3.1 %	485	200	200	0.18	4.6	S
	529	Tsonos (2007)	G1	Exterior	22.0	1.3 %	500	1.8 %	495	300	200	3.1 %	495	200	200	0.23	4.4	S-F
	530	Tsonos (2007)	A1	Exterior	35.0	1.0 %	540	1.2 %	500	300	200	1.6 %	500	200	200	0.14	4.4	S-F
	531	Tsonos (2007)	E2	Exterior	35.0	1.0 %	540	1.2 %	495	300	200	3.1 %	495	200	200	0.14	4.2	S-F
	532	Tsonos (2007)	E1	Exterior	22.0	1.0 %	540	1.8 %	495	300	200	3.1 %	495	200	200	0.23	5.9	S
139	533	Tsonos and Papanikolau (2003)	F2	Exterior	31.0	0.0 %	0	1.1 %	530	300	300	0.8 %	535	200	200	0.29	3.3	S
	534	Tsonos and Papanikolau (2003)	F1	Exterior	20.0	0.0 %	0	1.2 %	520	300	300	2.3 %	520	200	200	0.39	3.7	S-F
	535	Tsonos and Papanikolau (2003)	L1	Exterior	34.0	0.0 %	0	1.6 %	520	300	300	0.8 %	535	200	200	0.26	5.0	S
140	536	Tsonos et al. (1992)	P1	Exterior	16.0	0.0 %	0	2.2 %	485	300	200	3.1 %	485	200	200	0.18	3.1	S
	537	Tsonos et al. (1992)	V1	Exterior	23.0	0.0 %	0	2.2 %	485	300	200	3.1 %	485	200	200	0.18	3.5	S
	538	Tsonos et al. (1992)	F1	Exterior	17.0	0.0 %	0	2.2 %	485	300	200	3.1 %	485	200	200	0.18	4.4	S
141	539	Uzumeri (1977)	1	Exterior	30.8	0.0 %	0	2.1 %	332	508	305	2.8 %	331	381	381	0.41	5.0	S-F
	540	Uzumeri (1977)	5	Exterior	32.0	0.0 %	0	1.7 %	336	508	381	2.8 %	336	381	381	0.40	4.8	S-F
	541	Uzumeri (1977)	2	Exterior	31.1	0.0 %	0	2.1 %	349	508	305	2.8 %	335	381	381	0.41	4.6	S-F
	542	Uzumeri (1977)	6	Exterior	36.2	1.5 %	357	1.7 %	352	508	381	2.8 %	340	381	381	0.42	4.9	S-F
	543	Uzumeri (1977)	7	Exterior	30.8	0.9 %	365	1.7 %	352	508	381	2.8 %	340	381	381	0.52	4.8	S-F
	544	Uzumeri (1977)	8	Exterior	26.3	1.5 %	365	2.3 %	352	508	381	2.8 %	390	381	381	0.61	5.7	S-F
	545	Uzumeri (1977)	4	Exterior	31.0	0.9 %	380	2.1 %	349	508	305	2.8 %	333	381	381	0.42	5.1	S-F
	546	Uzumeri (1977)	3	Exterior	27.0	0.4 %	428	2.1 %	350	508	305	2.8 %	337	381	381	0.42	4.5	S-F
142	547	Walker (2001)	PEER14	Interior	31.8	0.0 %	0	1.9 %	423	508	406	1.4 %	423	457	406	0.11	5.2	S-F
	548	Walker (2001)	CD1514	Interior	29.8	0.0 %	0	1.9 %	423	508	406	1.4 %	423	457	406	0.12	5.4	S-F
	549	Walker (2001)	CD3014	Interior	42.5	0.0 %	0	1.9 %	423	508	406	1.4 %	423	457	406	0.08	6.2	S-F
	550	Walker (2001)	PADH14	Interior	42.9	0.0 %	0	1.9 %	423	508	406	1.4 %	423	457	406	0.08	6.5	S-F
	551	Walker (2001)	PEER22	Interior	38.4	0.0 %	0	2.6 %	527	508	406	2.8 %	538	457	406	0.09	7.4	S-F
	552	Walker (2001)	CD3022	Interior	38.1	0.0 %	0	2.6 %	516	508	406	2.8 %	510	457	406	0.09	7.9	S-F
	553	Walker (2001)	PADH22	Interior	36.3	0.0 %	0	2.6 %	527	508	406	2.8 %	538	457	406	0.10	7.9	S-F
143	554	Wang and Hsu (2009)	Ko-JII	Interior	31.7	0.0 %	0	3.2 %	533	500	300	3.4 %	533	300	300	0.14	8.5	S
	555	Wang and Hsu (2009)	Ho-JII	Interior	26.2	0.0 %	0	2.4 %	541	400	300	0.3 %	541	400	400	0.00	6.3	S
144	556	Wang and Lee (2004)	JE1	Exterior	20.0	0.0 %	0	2.0 %	520	400	300	2.5 %	461	400	400	0.00	2.9	S
145	557	Watanabe et al. (1998)	WJ-1	Interior	29.0	1.3 %	364	1.6 %	326	300	200	2.6 %	358	300	300	0.07	6.9	S-F
	558	Watanabe et al. (1998)	WJ-3	Interior	29.0	1.3 %	364	1.6 %	364	300	200	2.6 %	373	300	300	0.07	8.0	S-F
	559	Watanabe et al. (1998)	WJ-6	Interior	29.0	1.3 %	364	2.2 %	358	300	200	4.0 %	373	300	300	0.07	9.8	S-F
146	560	Wong (2005)	BS-L-600	Exterior	36.4	0.0 %	0	1.2 %	520	600	260	2.2 %	520	300	300	0.15	3.5	S

(continued on next page)



Table A1 (continued)

No. of studies	S.N	Research Studies	Specimen	Joint Type	$f'_c$ (MPa)	$\rho_{jt}$	$f_{jt}$ (MPa)	$\rho_b$	$f_{yb}$ (MPa)	$h_b$ (mm)	$b_b$ (mm)	$\rho_c$	$f_{yc}$ (MPa)	$h_c$ (mm)	$b_c$ (mm)	ALF	$\tau_{exp}$	Failure Mode
	561	Wong (2005)	JA-NN03	Exterior	44.8	0.0 %	0	1.4 %	520	450	260	2.2 %	520	300	300	0.03	3.6	S-F
	562	Wong (2005)	JA-NN15	Exterior	46.0	0.0 %	0	1.4 %	520	450	260	2.2 %	520	300	300	0.15	3.9	S-F
	563	Wong (2005)	BS-L	Exterior	30.9	0.0 %	0	1.6 %	520	450	260	2.2 %	520	300	300	0.15	3.8	S
	564	Wong (2005)	BS-LL	Exterior	42.1	0.0 %	0	1.6 %	520	450	260	2.2 %	520	300	300	0.15	4.8	S
	565	Wong (2005)	BS-L-LS	Exterior	31.6	0.0 %	0	1.6 %	520	450	260	2.2 %	520	300	300	0.15	4.1	S
	566	Wong (2005)	BS-L-V2T10	Exterior	32.6	0.0 %	0	1.6 %	520	450	260	2.2 %	520	300	300	0.15	4.7	S
	567	Wong (2005)	BS-L-V4T10	Exterior	28.3	0.0 %	0	1.6 %	520	450	260	2.2 %	520	300	300	0.15	4.8	S
	568	Wong (2005)	BS-U	Exterior	31.0	0.0 %	0	1.6 %	520	450	260	2.2 %	520	300	300	0.15	4.1	S
	569	Wong (2005)	JB-NN03	Exterior	47.4	0.0 %	0	2.1 %	520	300	260	2.2 %	520	300	300	0.03	4.4	S
	570	Wong (2005)	BS-L-300	Exterior	34.1	0.0 %	0	2.4 %	520	300	260	2.2 %	520	300	300	0.15	5.9	S
	571	Wong (2005)	BS-L-H1T10	Exterior	33.3	0.3 %	500	1.6 %	520	450	260	2.2 %	520	300	300	0.15	4.6	S
	572	Wong (2005)	BS-L-H2T10	Exterior	42.1	0.4 %	500	1.6 %	520	450	260	2.2 %	520	300	300	0.15	5.7	S
	573	Wong (2005)	JA-NY03	Exterior	34.9	0.5 %	500	1.5 %	520	400	260	2.2 %	520	300	300	0.03	3.6	S-F
	574	Wong (2005)	JA-NY15	Exterior	38.5	0.5 %	500	1.5 %	520	400	260	2.2 %	520	300	300	0.15	3.9	S-F
147	575	Wong and Kuang (2008)	BS-L-600	Exterior	36.4	0.0 %	0	1.3 %	520	600	260	2.4 %	520	300	300	0.31	3.1	S
	576	Wong and Kuang (2008)	BS-L-450	Exterior	30.9	0.0 %	0	1.7 %	520	450	260	2.4 %	520	300	300	0.36	3.5	S
	577	Wong and Kuang (2008)	BS-L-V2	Exterior	32.6	0.0 %	0	1.7 %	520	450	260	3.1 %	520	300	300	0.34	4.5	S
	578	Wong and Kuang (2008)	BS-L-V4	Exterior	28.3	0.0 %	0	1.7 %	520	450	260	3.7 %	520	300	300	0.39	4.5	S
	579	Wong and Kuang (2008)	BS-L-300	Exterior	34.1	0.0 %	0	2.6 %	520	300	260	2.4 %	520	300	300	0.33	5.6	S
	580	Wong and Kuang (2008)	BS-L-H1	Exterior	33.3	0.1 %	500	1.7 %	520	450	260	2.4 %	520	300	300	0.33	4.3	S
	581	Wong and Kuang (2008)	BS-L-H2	Exterior	42.1	0.1 %	500	1.7 %	520	450	260	2.4 %	520	300	300	0.26	5.3	S
148	582	Wong and Kuang (2011)	BS-600	Exterior	36.4	0.0 %	0	1.3 %	520	600	260	2.4 %	520	300	300	0.31	3.1	S
	583	Wong and Kuang (2011)	BS-450	Exterior	30.9	0.0 %	0	1.7 %	520	450	260	2.4 %	520	300	300	0.36	3.5	S
	584	Wong and Kuang (2011)	BS-600-H2T8	Exterior	41.8	0.1 %	500	1.3 %	520	600	260	2.4 %	520	300	300	0.27	4.0	S
	585	Wong and Kuang (2011)	BS-450-H1T10	Exterior	33.3	0.1 %	500	1.7 %	520	450	260	2.4 %	520	300	300	0.33	4.3	S
	586	Wong and Kuang (2011)	BS-600-H4T8	Exterior	29.7	0.3 %	500	1.3 %	520	600	260	2.4 %	520	300	300	0.37	3.8	S
	587	Wong and Kuang (2011)	BS-450-H2T10	Exterior	42.1	0.3 %	500	1.7 %	520	450	260	2.4 %	520	300	300	0.26	5.3	S
149	588	Yashita et al. (1996)	No. 1	Interior	43.1	0.4 %	823	3.9 %	409	395	300	2.0 %	409	415	415	0.10	8.1	S-F
	589	Yashita et al. (1996)	No. 3	Interior	54.3	0.4 %	823	3.2 %	405	395	300	2.0 %	405	415	415	0.10	9.4	S-F
	590	Yashita et al. (1996)	No. 4	Interior	53.8	0.4 %	823	3.2 %	702	395	300	2.0 %	702	415	415	0.10	11.6	S
150	591	Yoshino et al. (1997)	No. 1	Interior	28.6	0.5 %	420	1.3 %	382	250	180	2.5 %	379	250	250	0.16	7.2	S-F
	592	Yoshino et al. (1997)	No. 3	Interior	28.6	0.5 %	420	1.6 %	379	250	180	2.5 %	379	250	250	0.16	7.7	S-F
	593	Yoshino et al. (1997)	No. 4	Interior	28.6	0.5 %	420	1.1 %	379	250	180	2.5 %	379	250	250	0.16	6.3	S-F
151	594	Yoshiya et al. (1991)	No. 2	Interior	39.2	0.4 %	364	2.5 %	388	450	300	2.1 %	365	500	375	0.24	10.8	S-F
152	595	Zaid et al. (1999)	S3	Interior	28.0	0.5 %	390	1.9 %	470	300	200	3.8 %	450	300	300	0.04	8.8	S-F
153	596	Zhang and Li (2020)	EJ-0	Exterior	47.9	0.0 %	0	2.1 %	535	250	150	1.7 %	535	250	250	0.14	3.2	S-F
	597	Zhang and Li (2020)	EJ-2	Exterior	47.9	1.0 %	300	2.1 %	535	250	150	1.7 %	535	250	250	0.14	3.1	S-F
	598	Zhang and Li (2020)	EJ-4	Exterior	47.9	1.6 %	300	2.1 %	535	250	150	1.7 %	535	250	250	0.14	3.0	S-F

specimens compiled from 153 research studies. The first row of Table A1. presents the variables of the joint specimen where joint type is either interior or exterior;  $f'_c$  is the concrete compressive strength;  $\rho_{jt}$  is the joint transverse reinforcement ratio;  $f_{yjt}$  is the joint transverse reinforcement yield strength;  $\rho_b$  is the beam longitudinal reinforcement ratio;  $f_{yb}$  is the beam longitudinal reinforcement yield strength;  $b_b$  is the beam width;  $h_b$  is the beam depth;  $\rho_c$  is the column longitudinal reinforcement ratio;  $f_{yc}$  is the column longitudinal reinforcement yield strength;  $b_c$  is the column width;  $h_c$  the column depth; ALF is the axial load factor which equals to  $= P/fcph$  where P is the axial load of the column; and  $\tau_{exp}$  is the joint shear strength. Three types of failure modes are observed where 'S' denotes a joint shear failure, 'B' denotes a bond-slip failure; and 'S-F' denotes combination of joint shear and beam or column flexural failures at the joint interfaces. 97 specimens have missing or unreported failure modes which is denoted as 'unknown'.

## References

- Miani M, Marco CD, Frappa G, Pauletta M. Effects of dissipative systems on the seismic behavior of irregular buildings - Two case studies. *Build* 2020;10:1–27. <https://doi.org/10.3390/buildings10110202>.
- Hu B, Kundu T. Seismic performance of interior and exterior beam-column joints in recycled aggregate concrete frames. *J Struct Eng* 2019;145(3):16. [https://doi.org/10.1061/\(ASCE\)ST.1943-541X.0002261](https://doi.org/10.1061/(ASCE)ST.1943-541X.0002261).
- Clyde CP, Pantelides LD. Reaveley Performance-based evaluation of exterior reinforced concrete building joints for seismic excitation. PEER Report 2000. Pacific Earthquake Research Center, CA; 2000 [https://peer.berkeley.edu/sites/default/files/0005\\_c\\_clyde\\_c\\_pantelides\\_l\\_reaveley.pdf](https://peer.berkeley.edu/sites/default/files/0005_c_clyde_c_pantelides_l_reaveley.pdf).
- T. Paulay A. Scarpas The behavior of exterior beam-column joints. *Bulletin of the New Zealand National Society for Earthquake Engineering* 14 3 1981 131 144 [https://www.nzsee.org.nz/db/Bulletin/Archive/14\(3\)0131.pdf](https://www.nzsee.org.nz/db/Bulletin/Archive/14(3)0131.pdf).
- Shiohara H, Kusuhara F. Benchmark test for validation of mathematical models for non-linear and cyclic behavior of R/C beam-column joints. Department of Architecture: Graduate School of Engineering, University of Tokyo; 2007.
- Sasmal S, Lakshmanan N, Ramanjaneyulu K, Iyer NR, Novak Srinivas B, et al. Development of upgradation schemes for gravity load designed beam-column sub assemblage under cyclic loading. *Constr Build Mat* 2011;25(8):3625–38. <https://doi.org/10.1016/j.conbuildmat.2011.03.058>.
- Hwang SJ, Lee HJ, Liao TF, Wang KC, Tsai HH. Role of hoops on shear strength of reinforced concrete beam-column joints. *ACI Struct J* 2005;102(3):445–53. <https://doi.org/10.14359/14416>.
- ACI (American Concrete Institute). Building code requirements for structural concrete and commentary. ACI 318-19, Farmington Hills, MI: ACI; 2019.
- CSI (Computers and Structures, Inc.) SAP2000. Integrated software for structural analysis and design user's manual version 19, CSI, Berkeley, CA, USA; 2016 <https://docs.csiamerica.com/manuals/sap2000/CSIRefer.pdf>.
- Borghini A, Gusella F, Vignoli A. Seismic vulnerability of existing R.C. buildings: A simplified numerical model to analyze the influence of the beam-column joints collapse. *Eng Struct* 2016;121:19–29. <https://doi.org/10.1016/j.engstruct.2016.04.045>.
- Suwal N, Guner S. Nonlinear modeling of beam-column joints in forensic analysis of concrete buildings. *Comp Conc* 2023;31(5):14. <https://doi.org/10.12989/cac.2023.31.5.000>.
- Jeon JS. Aftershock vulnerability assessment of damaged reinforced concrete buildings in California. Atlanta: Georgia Institute of Technology; 2013. Ph.D. Dissertation.
- Birely AC, Lowes LN, Lehman DE. A model for the practical nonlinear analysis of reinforced-concrete frames including joint flexibility. *Eng Struct* 2012;34(1):455–65. <https://doi.org/10.1016/j.engstruct.2011.09.003>.
- Biddah A, Ghojarah A. Modelling of shear deformation and bond slip in reinforced concrete joints. *Struct Eng Mech* 1999;7(4):413–32. <https://doi.org/10.12989/sem.1999.7.4.413>.
- Ghojarah A, Biddah A. Dynamic analysis of reinforced concrete frames including joint shear deformation. *Eng Struct* 1999;21(11):971–87. [https://doi.org/10.1016/S0141-0296\(98\)00052-2](https://doi.org/10.1016/S0141-0296(98)00052-2).
- Alath S, Kunnath SK. Modeling inelastic shear deformations in RC beam-column joints. *Engineering Mechanics: Proceedings of 10th Conference, The University of Colorado at Boulder* 3 1995 822 825.
- Mitra N, Lowes LN. Evaluation, calibration, and verification of a reinforced concrete beam-column joint model. *J Struct Eng* 2007;133(1):105–20. [https://doi.org/10.1061/\(ASCE\)0733-9445](https://doi.org/10.1061/(ASCE)0733-9445).
- Shin M, Lafave JM. Modeling of cyclic joint shear deformation contributions in RC beam-column connections to overall frame behavior. *Struct Eng Mech* 2004;18(5):645–69. <https://doi.org/10.12989/sem.2004.18.5.645>.
- Lowes LN, Altoontash A. Modeling reinforced-concrete beam-column joints subjected to cyclic loading. *J Struct Eng* 2003;129(12):1686–97. [https://doi.org/10.1061/\(ASCE\)0733-9445\(2003\)](https://doi.org/10.1061/(ASCE)0733-9445(2003)).
- Youssef M, Ghojarah A. Modelling of RC beam-column joints and structural walls. *J Earthq Eng* 2001;5(1):93–111. <https://doi.org/10.1080/13632460109350387>.
- S. Guner FJ. Vecchio Analysis of shear-critical reinforced concrete plane frame elements under cyclic loading. *J Struct Eng* 137 8 2011 834 843 <https://ascelibrary.org/doi/abs/10.1061/%28ASCE%29ST.1943-541X.0000346>.
- Eligehausen R, Ozbolt J, Genesio G, Hoehler MS, Pampanin S. Three-dimensional modeling of poorly detailed RC frame joints. In *Proceedings of the Annual NZSEE Conference, New Zealand* 23 2006 10pp.
- SA. Almeida S. Guner Review of artificial neural network and a new feed-forward network for anchorage analysis in cracked concrete *Conc Indus Era AI, ACI* 2021; SP-350(5):54-68 [https://www.utoledo.edu/engineering/faculty/serhan-guner/docs/JP23\\_Almeida\\_Guner\\_AI\\_Concrete\\_2021.pdf](https://www.utoledo.edu/engineering/faculty/serhan-guner/docs/JP23_Almeida_Guner_AI_Concrete_2021.pdf).
- Kotsouvo GM, Costovos DM, Lagaros ND. Assessment of RC exterior beam-column joints based on artificial neural networks and other methods. *Eng Struct* 2017;144:1–18. <https://doi.org/10.1016/j.engstruct.2017.04.048>.
- EN 1992-1. Eurocode 2: Design of concrete structures – Part 1-1: General rules, and rules for buildings, London; 2004.
- EN 1998-1. Eurocode 8: Design of structures for earthquake resistance – Part 1-1: General rules, seismic actions, and rules for buildings, London; 2004.
- Gao X, Lin C. Prediction model of the failure mode of beam-column joints using machine learning methods. *Eng Fail Anal* 2021;120(1239). <https://doi.org/10.1016/j.engfailanal.2020.105072>.
- Alagundi S, Palanisamy T. Neural network prediction of joint shear strength of exterior beam-column joint. *Struct* 2022;37:1002–18. <https://doi.org/10.1016/j.istruc.2022.01.013>.
- Haido JH. Prediction of the shear strength of RC beam-column joints using new ANN formulations. *Struct* 2022;38:1191–209. <https://doi.org/10.1016/j.istruc.2022.02.046>.
- Marie HS, El-Hassan KA, Almetwally EM, El-Mandouh MA. Joint shear strength prediction of beam-column connections using machine learning via experimental results. *Case Stud Const Mater* 2022;17:1–17. <https://doi.org/10.1016/j.cscm.2022.e01463>.
- Almeida SA, Guner S. A hybrid methodology using finite elements and neural network for the analysis of adhesive anchors exposed to hurricanes and adverse environments. *Eng Struct* 2020;212:9.
- Gesoglu M, Güneysi E. Prediction of load-carrying capacity of adhesive anchors by soft computing techniques. *Mater and Struct* 2007;40:939–51. <https://doi.org/10.1617/s11527-007-9265-6>.
- Ashour AF, Alqedra MA. Concrete breakout strength of single anchors in tension using neural networks. *Adv Eng Soft* 2005;36:87–97. <https://doi.org/10.1016/j.advengsoft.2004.08.001>.
- Qian N. On the momentum term in gradient descent learning algorithms. *Neur Netw* 1999;12(1):145–51. [https://doi.org/10.1016/S0893-6080\(98\)00116-6](https://doi.org/10.1016/S0893-6080(98)00116-6).
- Kingma DP, Ba JL. Adam: A method for stochastic optimization. The 3rd international conference for learning representations. San Diego 2015;15.
- Hinton G, Srivastava N, Swersky K. Neural networks for machine learning. Coursera, video lectures 2012;264:41.
- Abadi M, Agarwal A, Barham P, Brevedo E, Chen Z, Citro C et al. Tensorflow (v2.10.0): Large-scale machine learning on heterogeneous systems software 2015. <https://www.tensorflow.org/>.
- Rossum G, Drake Jr FL. Python reference manual. Amsterdam, Netherlands: Center for Mathematics and Computer Science; 1995.
- Cook RD. Influential observations in linear regression. *J Amer Stat Assoc* 1979;74(365):169–74. <https://doi.org/10.1080/01621459.1979.10481634>.
- Cook RD. Detection of influential observation in linear regression. *Techno* 1977;19(1):15–8. <https://doi.org/10.2307/1268249>.
- Lazaridis PC, Kavvadias IE, Demertzis K, Iliadis L, Vasilidiadis LK. Structural damage prediction of a reinforced concrete frame under single and multiple seismic events using machine learning algorithms. *Appl Sci* 2022;12(8):22. <https://doi.org/10.3390/app12083845>.
- Schober P, Boer C, Schwarte LA. Correlation coefficients. *Anesth Analg* 2018;126(5):1763–8. <https://doi.org/10.1213/ane.0000000000002864>.
- Etikan I, Bala K. Sampling and sampling methods. *Biome Biostat Intl J* 2017;5(6):3. <https://doi.org/10.15406/bbij.2017.05.00149>.
- Kumari K, Mrunalini M. Detecting denial of service attacks using machine learning algorithm. *J Big Data* 2022;9(56):17. <https://doi.org/10.1186/s40537-022-00616-0>.
- Mori M, Flores RG, Suzuki Y, Nukazawa K, Hiraoka T, Nonaka H. Prediction of microcystis occurrences and analysis using machine learning in high-dimension, low sample-size, and imbalanced water quality data. *Harm Algae* 2022;117:14. <https://doi.org/10.1016/j.hal.2022.126273>.
- Park S. Experimental and analytical studies on old reinforced concrete buildings with seismically vulnerable beam-column joints. Berkeley: University of California; 2010. Ph.D. Dissertation.
- Kim J, LaFave JM. Joint shear behavior of reinforced concrete beam-column connections subjected to seismic lateral loading. Urbana Champaign, USA: Department of Civil and Environmental Engineering, University of Illinois at; 2009. Newmark Structural Laboratory Report Series.
- Guner S. Performance assessment of shear-critical reinforced concrete plane frames. Toronto, Canada: University of Toronto; 2008. Ph.D. Dissertation.
- Anderson M, Lehman D, Santon J. A cyclic shear stress-strain model for joints without transverse reinforcement. *Eng Struct* 2008;30(4):941–54. <https://doi.org/10.1016/j.engstruct.2007.02.005>.

- [50] Celik OC, Ellingwood BR. Modeling beam-column joints in fragility assessment of gravity load designed reinforced concrete frames. *J Earthq Eng* 2008;12(3): 357–81. <https://doi.org/10.1080/13632460701457215>.
- [51] Suwal N, Guner S. Beam-column joint hinge generator using an artificial neural network. Excel spreadsheet. Department of Civil and Environmental Engineering, University of Toledo, OH, USA; 2023. <[www.utoledo.edu/engineering/faculty/serhan-guner/docs/8S-ANNJointHingeGenerator.xlsx](http://www.utoledo.edu/engineering/faculty/serhan-guner/docs/8S-ANNJointHingeGenerator.xlsx)>.
- [52] Suwal N, Guner S. User Bulletin 11: Joint hinge generator spreadsheet using an artificial neural network. Documentation. Department of Civil and Environmental Engineering: University of Toledo, OH, USA; 2023. p. 6.